The Particle-Hole Map: a computational tool to visualize electronic excitations

Carsten A. Ullrich
University of Missouri

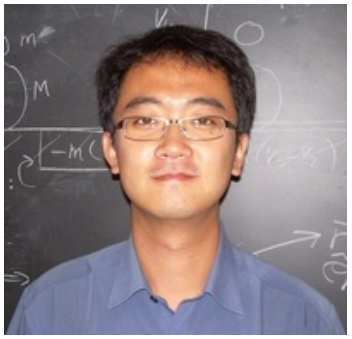

Yonghui Li
Tianjin University

Benasque
September 22, 2016

Outline

- **Visualization/interpretation methods of electronic excitations**
- **The particle-hole map: definitions**
- **Examples and applications**

Y. Li and C.A. Ullrich, Chem. Phys. **391**, 157 (2011)
Y. Li and C.A. Ullrich, J. Chem. Theory Comput. **11**, 5838 (2016)
Y. Li, D. Moghe, S. Patil, S. Guha, and C.A. Ullrich, Mol. Phys. **114**, 1365 (2016)
Y. Li and C.A. Ullrich, submitted to JCP (2016)

Molecular optical spectroscopy

- Uses (weak) laser as Probe
- System Response has peaks at electronic excitation energies
- Spectra can be calculated using TDDFT

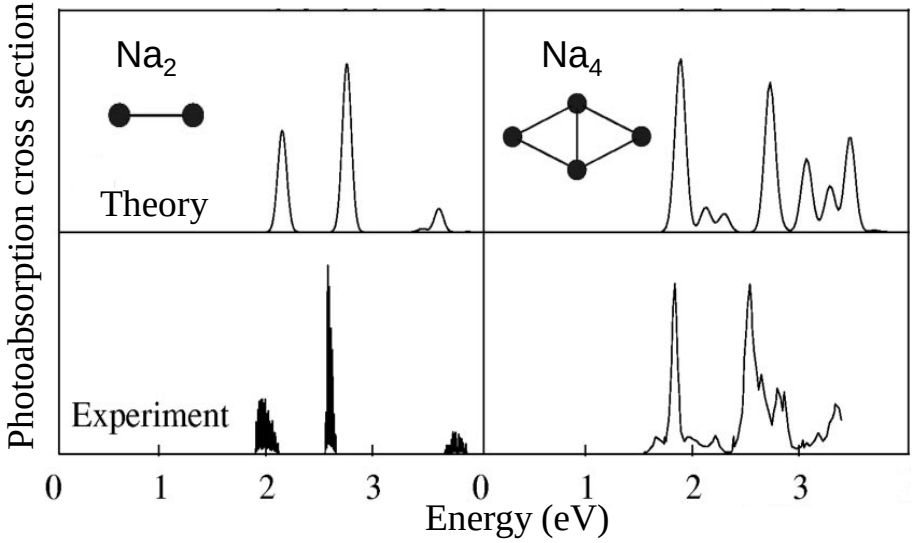

Vasiliev et al., PRB **65**, 115416 (2002)

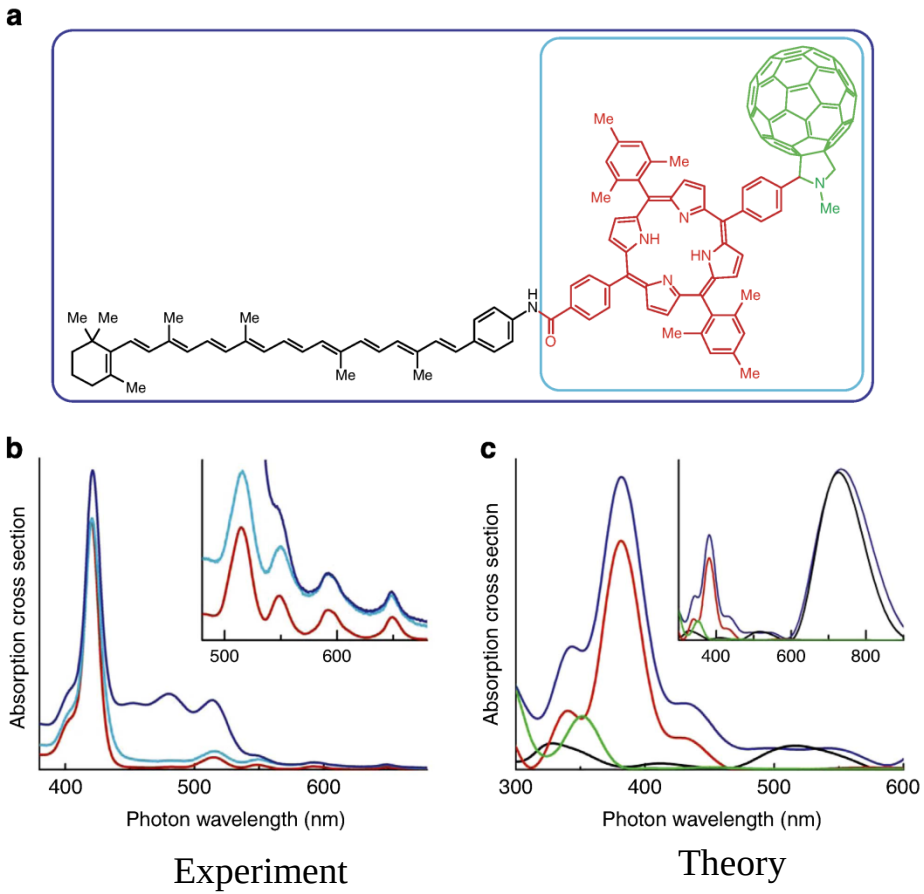

Rozzi et al., Nature Commun. (2013)

Real-time simulation of exciton dynamics

- Would like to visualize e-h pair motion in real time
- CT exciton creation, diffusion, dissociation at D-A interfaces
- important for understanding organic photovoltaics systems

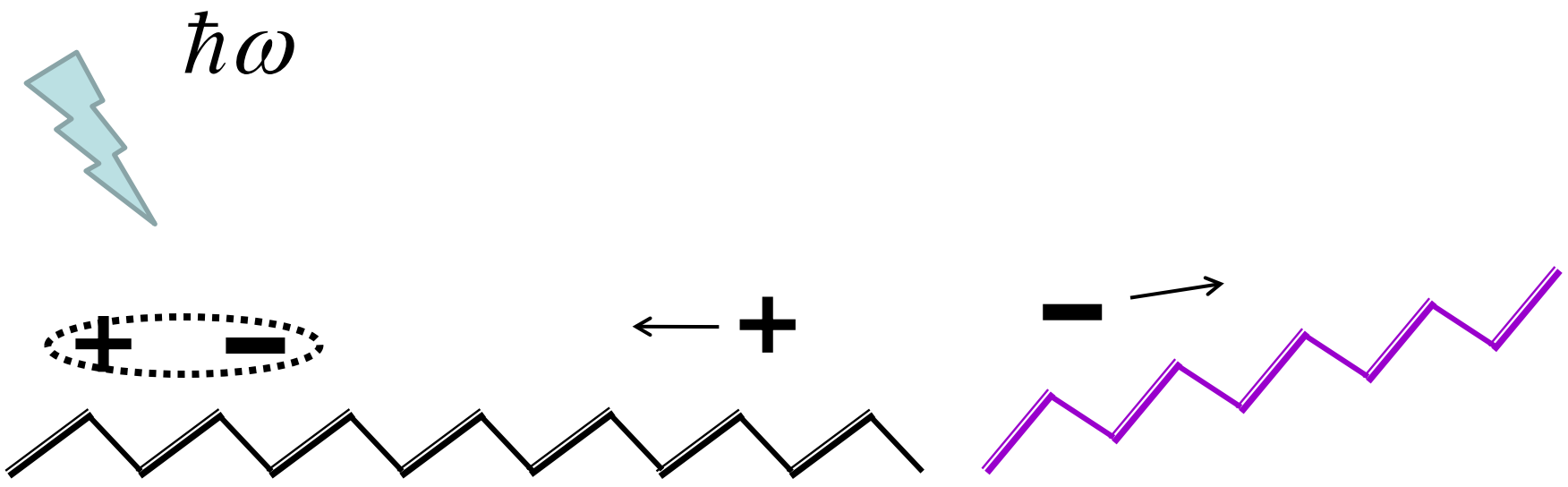

Real-time simulation of exciton dynamics

- **Would like to visualize e-h pair motion in real time**
- **CT exciton creation, diffusion, dissociation at D-A interfaces**
- **important for understanding organic photovoltaics systems**
- **Real D-A systems are complex, and require taking lattice relaxation into account.**
- **What should we be looking at?**

Semiconducting polymer (donor)

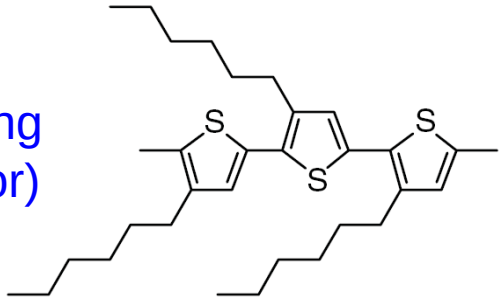

e-

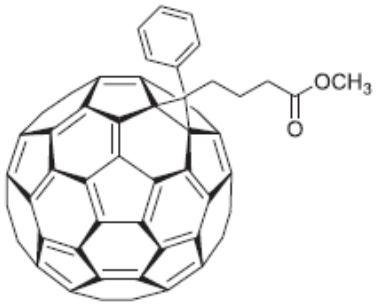

Fullerene (acceptor)

Charge-transfer excitations

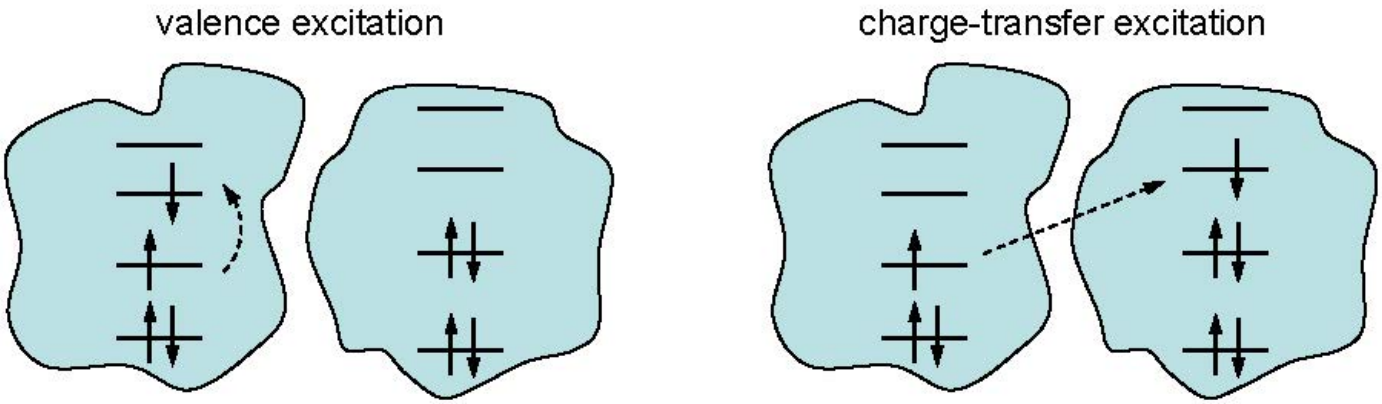

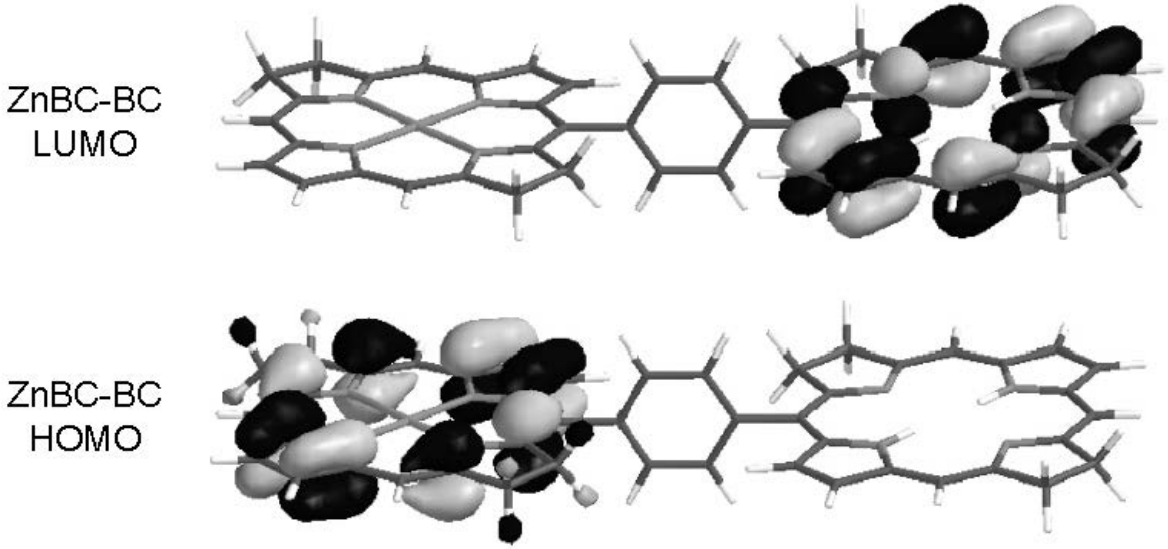

Zincbacteriochlorin-Bacteriochlorin complex (light-harvesting in plants and purple bacteria)

CT excitations are difficult with TDDFT: LDA and GGA fail.

Dreuw and Head-Gordon, JACS (2004)

Transition densities and difference densities

Example: MEH-PPV Li *et al*, Comp. Mat. Sci. **39**, 575 (2007)

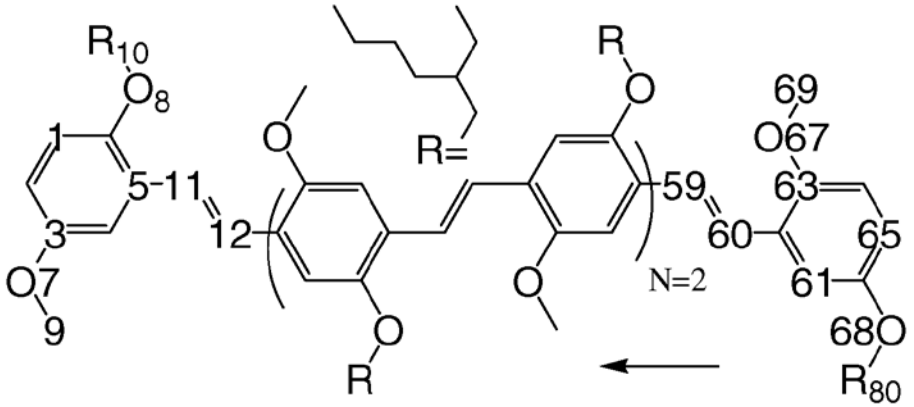

transition density (lowest excited state)

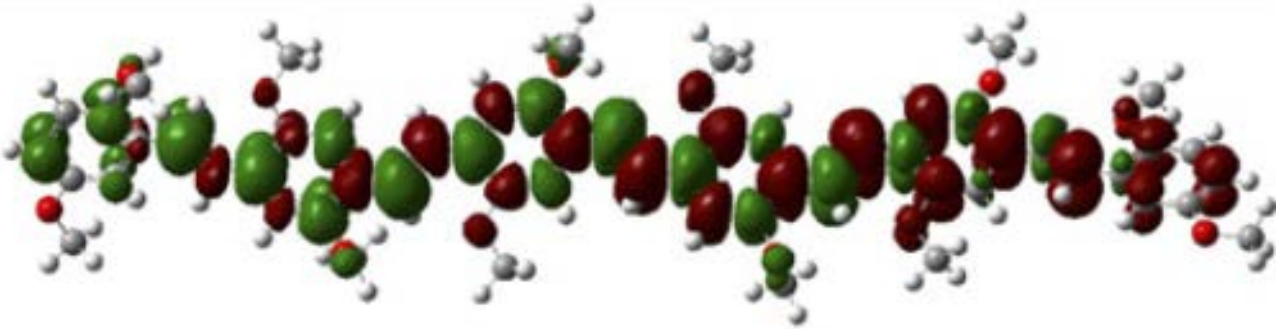

charge density difference

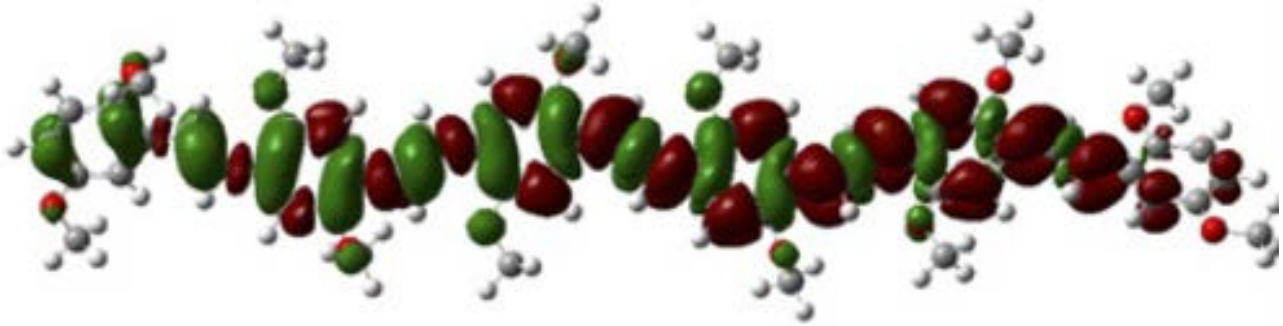

Visualization of electron dynamics: TDELF

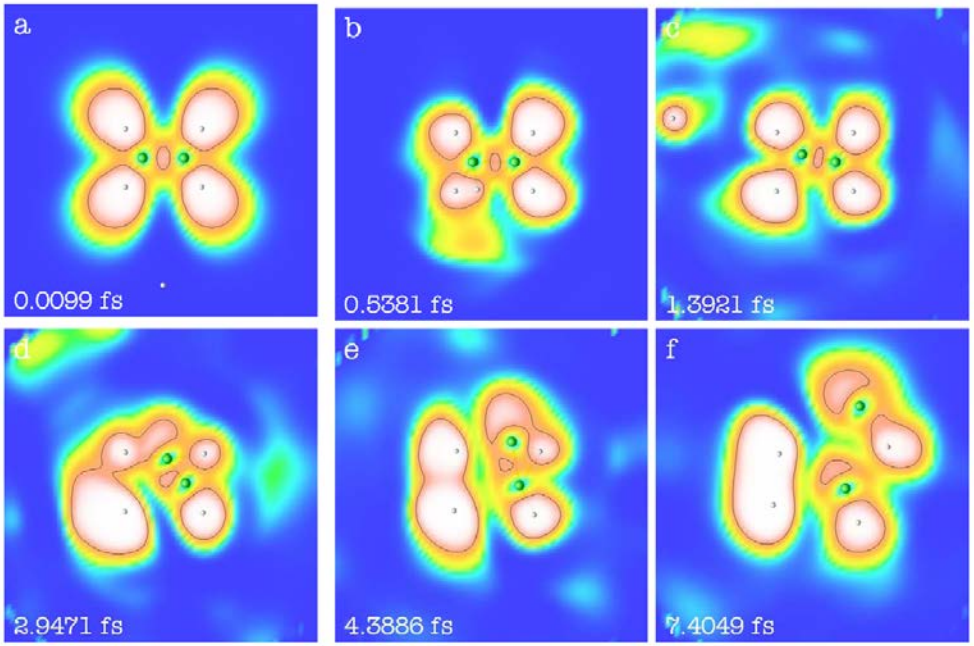

$$f_{ELF}(\mathbf{r},t) = \frac{1}{1+[D_\sigma(\mathbf{r},t)/D_\sigma^0(\mathbf{r},t)]^2}$$

$$D_\sigma(\mathbf{r},t) = \tau_\sigma(\mathbf{r},t) - \frac{|\nabla n_\sigma(\mathbf{r},t)|^2}{8n_\sigma(\mathbf{r},t)} - \frac{|\mathbf{j}_\sigma(\mathbf{r},t)|^2}{2n_\sigma(\mathbf{r},t)}$$

Time-Dependent Electron Localization Function (TDELF)
T. Burnus, M.A.L. Marques, E.K.U. Gross, PRA **71**, 010501(R) (2005)

- **Local** quantities like TDELF or the density itself show the motion of charges and ions or the breaking of bonds
- Charge fluctuations can be seen from transition densities or density differences, charge transfer can often be seen from MO's
- But where do electrons and holes come from or go to? How do we identify electron-hole pairs or excitons? **Need nonlocal information.**

Electron-hole distributions for exciton

LiF

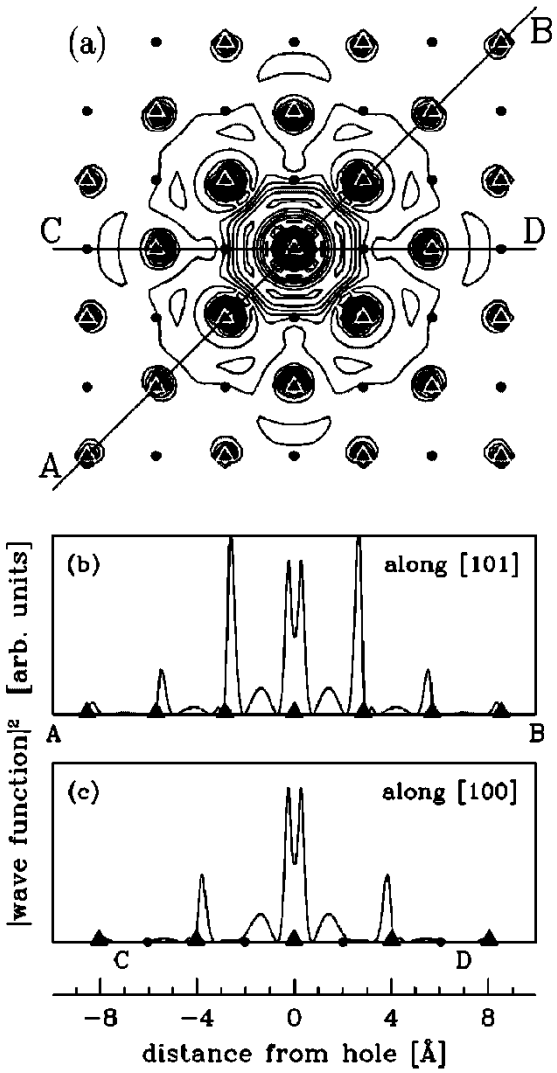

Rohlfing and Louie,
PRB **62**, 4927 (2000)

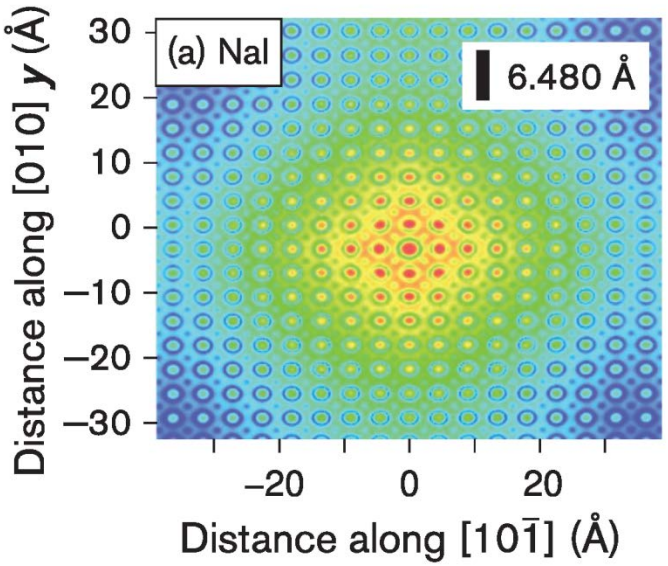

Erhart, Schleife, Sadigh and
Aberg, PRB **89**, 075132 (2014)

Obtained from solutions of
the GW-Bethe-Salpeter eq.

Transition Density Matrix (TDM)

TDM associated with a specific excitation $\Psi_0 \rightarrow \Psi_n$:

$$\Gamma_n(\mathbf{r},\mathbf{r}') = \left\langle \Psi_n \left| \hat{\rho}(\mathbf{r},\mathbf{r}') \right| \Psi_0 \right\rangle$$

Many-body eigenstates: $\hat{H}_0 \Psi_n = E_n \Psi_n$

1-body density matrix operator: $\hat{\rho}(\mathbf{r},\mathbf{r}') = \hat{\psi}^+(\mathbf{r}')\hat{\psi}(\mathbf{r})$

R. McWeeny, RMP **32**, 335 (1960)
F. Furche, JCP **114**, 5982 (2001)

Diagonalizing the TDM in a basis of natural orbitals gives the natural transition orbitals. R.L. Martin, JCP **118**, 4775 (2003).

TDDFT formalism for excitation energies

Excitation energies follow from eigenvalue problem (Casida 1995):

$$\begin{pmatrix} \mathbf{A} & \mathbf{K} \\ \mathbf{K}^* & \mathbf{A}^* \end{pmatrix} \begin{pmatrix} \mathbf{X} \\ \mathbf{Y} \end{pmatrix} = \Omega_n \begin{pmatrix} -\mathbf{1} & \mathbf{0} \\ \mathbf{0} & \mathbf{1} \end{pmatrix} \begin{pmatrix} \mathbf{X} \\ \mathbf{Y} \end{pmatrix}$$

$$A_{ia,i'a'} = \delta_{ii'}\delta_{aa'}\left(\varepsilon_a - \varepsilon_i\right) + K_{ia,i'a'}$$

$$K_{ia,i'a'} = \int d^3r \int d^3r' \varphi_i^*(\mathbf{r})\varphi_a(\mathbf{r})\left[\frac{1}{|\mathbf{r}-\mathbf{r}'|} + f_{xc}(\mathbf{r},\mathbf{r}',\omega)\right]\varphi_{i'}(\mathbf{r}')\varphi_{a'}(\mathbf{r}')$$

transition density:

$$\delta n(\mathbf{r},\Omega_n) = \sum_{ia}\left[\varphi_i(\mathbf{r})\varphi_a^*(\mathbf{r})X_{ia}(\Omega_n) + \varphi_i^*(\mathbf{r})\varphi_a(\mathbf{r})Y_{ia}(\Omega_n)\right]$$

Kohn-Sham TDM

S. Tretiak and S. Mukamel, Chem. Rev. **102**, 3171 (2002)
F. Furche, JCP **114**, 5982 (2001)
F. Plasser, M. Wormit and A. Dreuw, JCP **141**, 024106 (2014)

$$\Gamma_n^{KS}(\mathbf{r},\mathbf{r}') = \sum_{ia}\left[\varphi_a^*(\mathbf{r})\varphi_i(\mathbf{r}')X_{ia}(\Omega_n) + \varphi_i^*(\mathbf{r})\varphi_a(\mathbf{r}')Y_{ia}(\Omega_n)\right]$$

The diagonal elements are (in principle) exact transition densities:

$$\Gamma_n^{KS}(\mathbf{r},\mathbf{r}) = \Gamma_n(\mathbf{r},\mathbf{r}) = \delta n(\mathbf{r},\Omega_n)$$

The off-diagonal elements are in general **not** exact:

$$\Gamma_n^{KS}(\mathbf{r},\mathbf{r}') \neq \Gamma_n(\mathbf{r},\mathbf{r}'), \quad \mathbf{r} \neq \mathbf{r}'$$

Time-dependent TDM

Y. Li and C.A. Ullrich, Chem. Phys. **391**, 157 (2011)

$$\Gamma(\mathbf{r},\mathbf{r}',t) = \left\langle \Psi(t) \middle| \hat{\rho}(\mathbf{r},\mathbf{r}') \middle| \Psi_0 e^{-iE_0 t} \right\rangle$$

KS Time-dependent TDM:

$$\Gamma^{KS}(\mathbf{r},\mathbf{r}',t) = \left\langle \Phi(t) \middle| \hat{\rho}(\mathbf{r},\mathbf{r}') \middle| \Phi_0 e^{-iE_0^{KS} t} \right\rangle$$

Where $\Phi(t), \Phi_0$ are time-dependent and ground-state Kohn-Sham Slater determinants:

$$\Phi(t) = \det\left\{\varphi_j(r,t)\right\} \qquad \left(-\frac{\nabla^2}{2} + v(t) + v_H(t) + v_{xc}(t)\right)\varphi_j(t) = i\frac{\partial}{\partial t}\varphi_j(t)$$

TDM for low-energy excited states of PPV_{10}

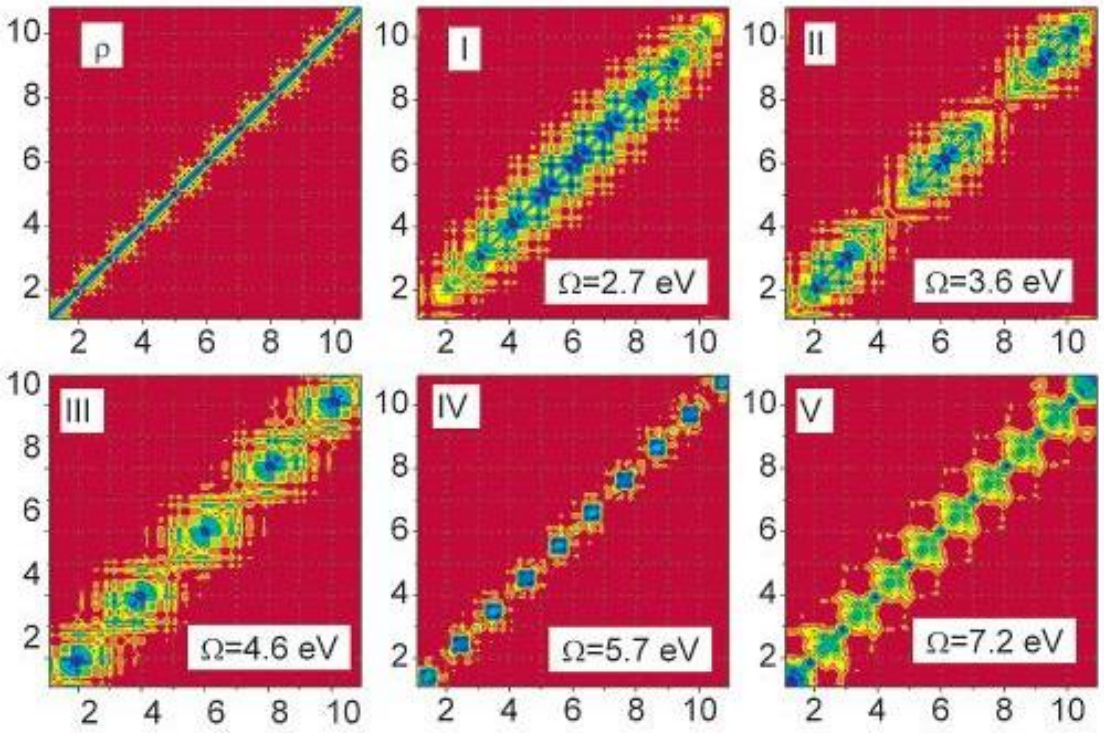

TDHF calculation

S.Tretiak, and S.Mukamel,
Chem. Rev. **102**, 3171 (2002)

S. Tretiak, K. Igumenshchev, and
S. Mukamel, PRB **71**, 033201 (2005)

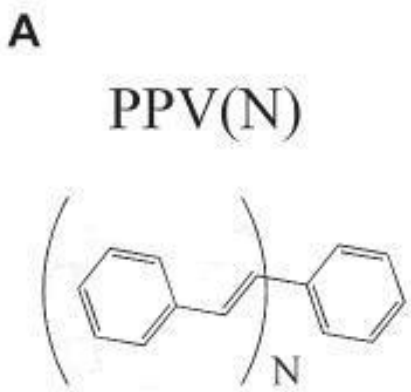

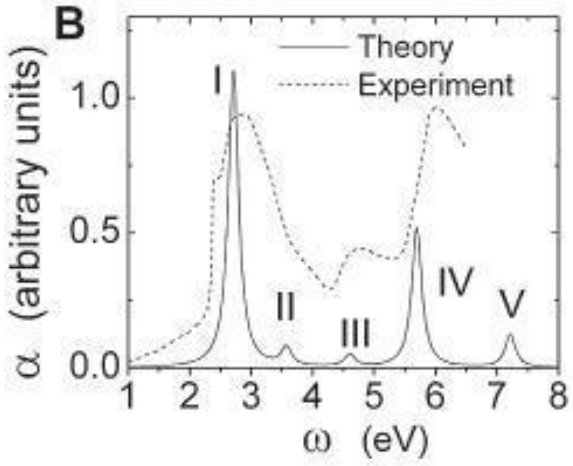

Two characteristic length scales

Coherence Length L_c

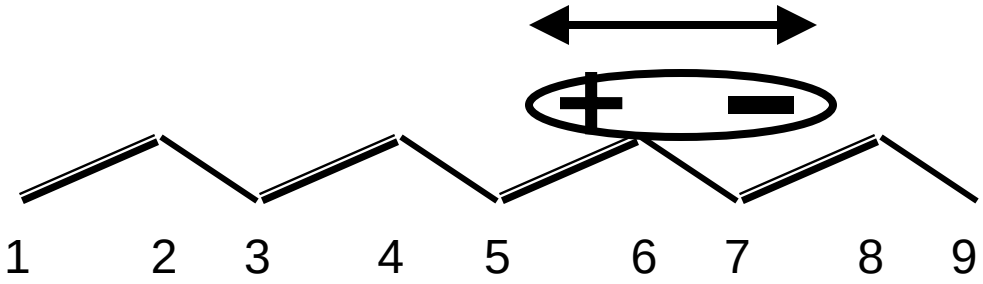

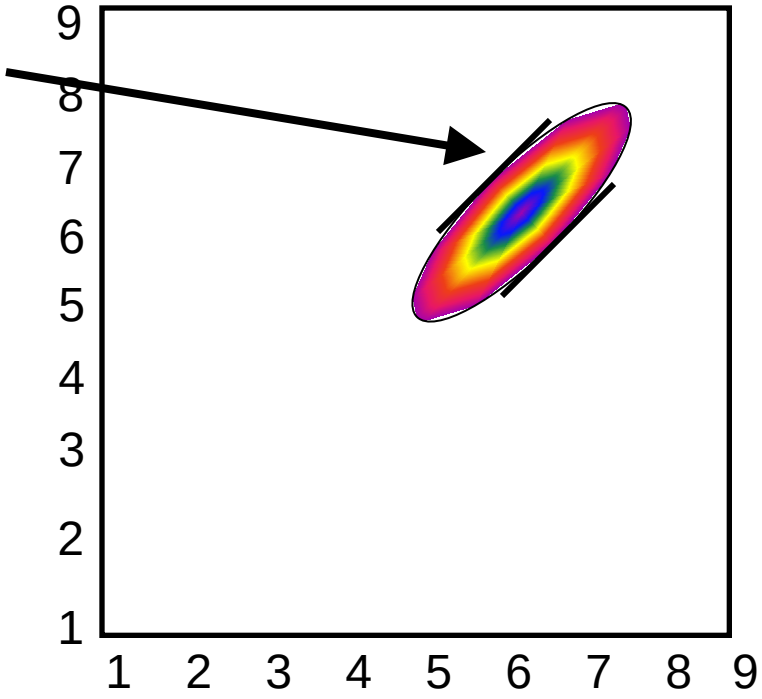

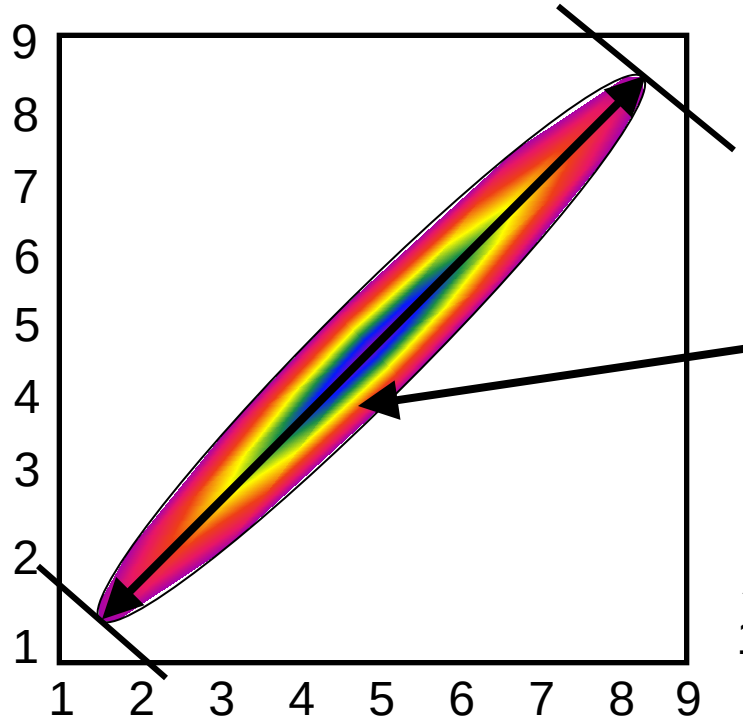

Delocalization Length L_d

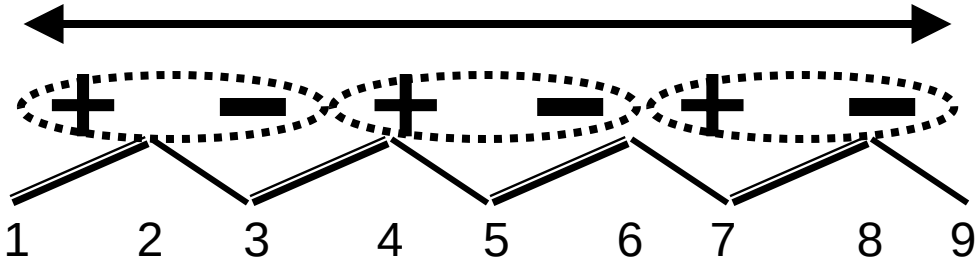

TDM for low-energy excited states of PPV_{20}

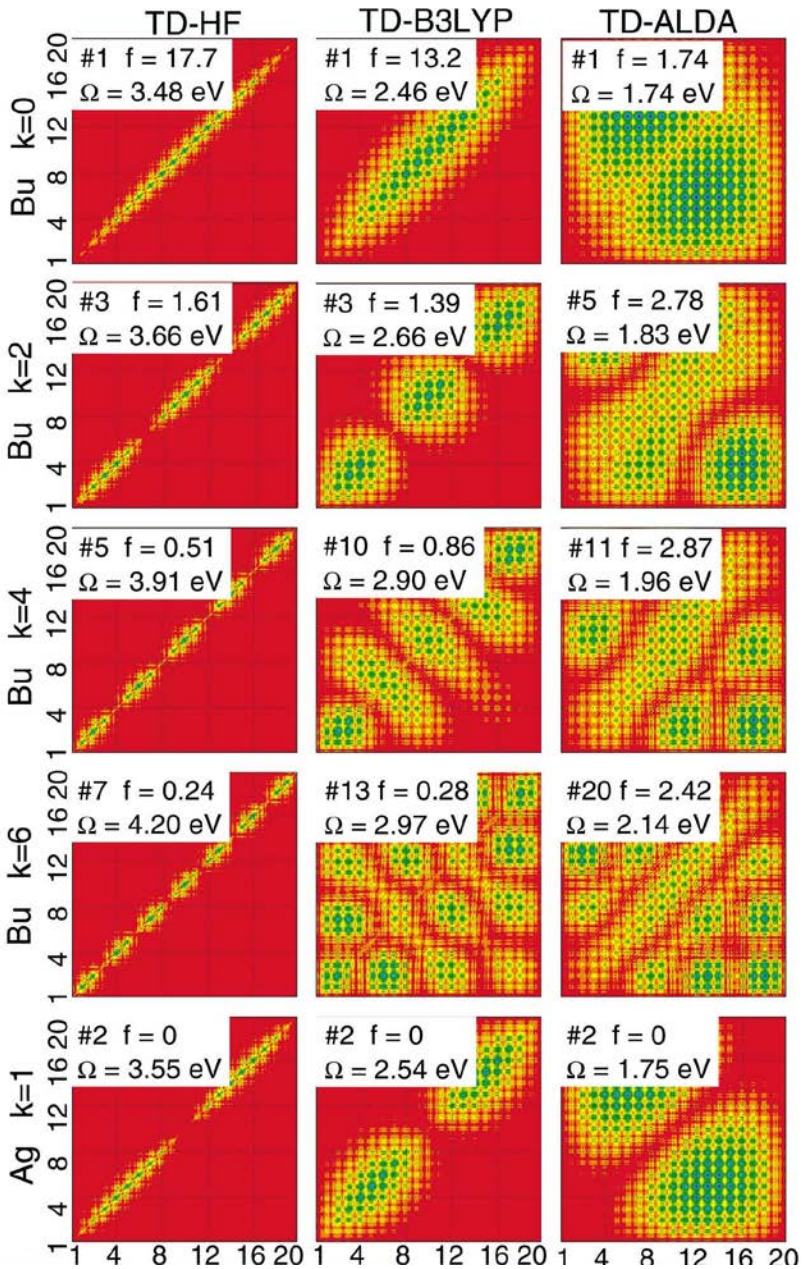

S. Tretiak, K. Igumenshchev, and S. Mukamel, PRB **71**, 033201 (2005)

- ► TDHF gives overbound excitons
- ►No bound excitons in ALDA (e-h repulsion)
- ►Hybrid functionals have bound excitons

Transition Density Matrix

- TDM is easy to compute and represent
- Allows to visualize excitonic character of an excitation (= electron-hole wave function)
- The TDM does not tell us where electron and hole are coming from: difficult to assess charge-transfer character of an excitation
- New visualization tool, complementary to TDM: the particle-hole map (PHM)

The time-dependent particle-hole map (I)

TDKS equation:

$$i\hbar\frac{\partial}{\partial t}\varphi_j(\mathbf{r},t)=\left[-\frac{\hbar^2\nabla^2}{2m}+V_s(\mathbf{r},t)\right]\varphi_j(\mathbf{r},t)$$

where

$$\varphi_j(\mathbf{r},t=0)=\varphi_j^{(0)}(\mathbf{r}),\qquad j=1,\ldots,N$$

Consider the following sum of joint probabilities:

$$P(\mathbf{r},\mathbf{r}',t)=\sum_{i=1}^{N}\left\{|\,\varphi_i(\mathbf{r}',t)\,|^2-|\,\varphi_i^{(0)}(\mathbf{r}')\,|^2\right\}|\,\varphi_i^{(0)}(\mathbf{r})\,|^2$$

density fluctuation of ith time-dependent KS orbital

ground-state probability density of ith KS orbital at position $\mathbf{r}$

The time-dependent particle-hole map (II)

For small perturbation, we can linearize:

$$|\varphi_i(\mathbf{r}',t)|^2 - |\varphi_i^{(0)}(\mathbf{r}')|^2$$

$$= \varphi_i^{(0)}(\mathbf{r}')\delta\varphi_i(\mathbf{r}',t) + c.c.$$

$$= \varphi_i^{(0)}(\mathbf{r}')\delta\varphi_{i,o}(\mathbf{r}',t) + \varphi_i^{(0)}(\mathbf{r}')\delta\varphi_{i,u}(\mathbf{r}',t) + c.c.$$

where the orbital fluctuations involving initially unoccupied states are obtained by projection:

$$\delta\varphi_{i,u}(\mathbf{r}',t) = \varphi_i(\mathbf{r}',t) - \sum_{i=1}^{N} \varphi_j^{(0)}(\mathbf{r}') \int d^3r'' \varphi_i(\mathbf{r}'',t)\varphi_i^{(0)}(\mathbf{r}'')$$

The orbital fluctuations involving occupied states don't contribute to the linear density response are and hence discarded

The time-dependent particle-hole map (III)

$$\Xi(\mathbf{r},\mathbf{r}',t)=\sum_{i=1}^{N}\left\{\varphi_i^{(0)}(\mathbf{r}')\delta\varphi_{i,u}(\mathbf{r}',t)+c.c.\right\}|\,\varphi_i^{(0)}(\mathbf{r})\,|^2$$

Sum of joint probability densities that a KS particle originates at position **r** and moves, during the excitation process, to position **r'**.

$$\Xi(\mathbf{r},\mathbf{r}',t\le 0)=0 \qquad \text{(starting from ground state)}$$

$$\int \Xi(\mathbf{r},\mathbf{r}',t)d^3r'=0 \qquad \text{(norm conservation)}$$

$$\int \Xi(\mathbf{r},\mathbf{r}',t)d^3r=\delta n(\mathbf{r}',t) \qquad \text{(exact density response)}$$

The frequency-dependent particle-hole map

We expand $$\delta\varphi_{i,u}(\mathbf{r},t) = \sum_{a=N+1}^{\infty} C_{ia}(t)\varphi_a^{(0)}(\mathbf{r})e^{i\omega_{ia}t}$$

If the system is in the electronic eigenmode of the nth excited state,

$$\delta n(\mathbf{r},t) = e^{-i\Omega_n t}\delta n(\mathbf{r},\Omega_n)$$

Using sum rule and comparing with the Casida equation from TDDFT,

$$\Xi(\mathbf{r},\mathbf{r}',\Omega_n) =$$

$$\sum_{ia}\left[\varphi_i^{(0)}(\mathbf{r}')\varphi_a^{(0)*}(\mathbf{r}')X_{ia}(\Omega_n) + \varphi_i^{(0)*}(\mathbf{r}')\varphi_a^{(0)}(\mathbf{r}')Y_{ia}(\Omega_n)\right]|\varphi_i^{(0)}(\mathbf{r})|^2$$

Derivation from 2-particle RDM (I)

2nd-order particle-hole transition density matrix between two Slater determinants:

$$\gamma_2^{ph}(ia,0;\mathbf{r}_1,\mathbf{r}_2;\mathbf{r}_1',\mathbf{r}_2')$$

$$= \left\langle \Phi_{ia} \left| \hat{\psi}^+(\mathbf{r}_1')\hat{\psi}(\mathbf{r}_2')\hat{\psi}^+(\mathbf{r}_2)\hat{\psi}(\mathbf{r}_1) \right| \Phi_0 \right\rangle$$

$$= \varphi_i(\mathbf{r}_1)\varphi_a^*(\mathbf{r}_1')\bar{\gamma}_1(\mathbf{r}_2',\mathbf{r}_2) - \gamma_1(\mathbf{r}_1,\mathbf{r}_1')\varphi_i(\mathbf{r}_2')\varphi_a^*(\mathbf{r}_2)$$

$$+ \varphi_i(\mathbf{r}_2)\varphi_a^*(\mathbf{r}_1)\gamma_1(\mathbf{r}_2',\mathbf{r}_1') + \gamma_1(\mathbf{r}_1,\mathbf{r}_2)\varphi_i(\mathbf{r}_2')\varphi_a^*(\mathbf{r}_1')$$

Derivation from 2-particle RDM (II)

Projection onto occupied KS orbitals: $P_l(\mathbf{r},\mathbf{r}') = \varphi_l(\mathbf{r})\varphi_l^*(\mathbf{r}')$

$$\sum_l^{occ} \left\langle P_l \left| \gamma_2^{ph}(ia,0) \right| P_l \right\rangle (\mathbf{r}',\mathbf{r}';\mathbf{r},\mathbf{r}) = \varphi_i(\mathbf{r}')\varphi_a^*(\mathbf{r}') \,|\, \varphi_i(\mathbf{r}) \,|^2$$

$$\Xi(\mathbf{r},\mathbf{r}',\Omega_n) = \sum_l^{occ} \left\langle P_l \left| \gamma_2^{ph}(\Omega_n) \right| P_l \right\rangle (\mathbf{r}';\mathbf{r})$$

$$= \sum_{ia} \left[\varphi_i(\mathbf{r}')\varphi_a^*(\mathbf{r}') X_{ia}(\Omega_n) + \varphi_i^*(\mathbf{r}')\varphi_a(\mathbf{r}') Y_{ia}(\Omega_n) \right] |\, \varphi_i(\mathbf{r}) \,|^2$$

PHM: orbital-projected particle-hole 2-TDM

PHM: 1D examples

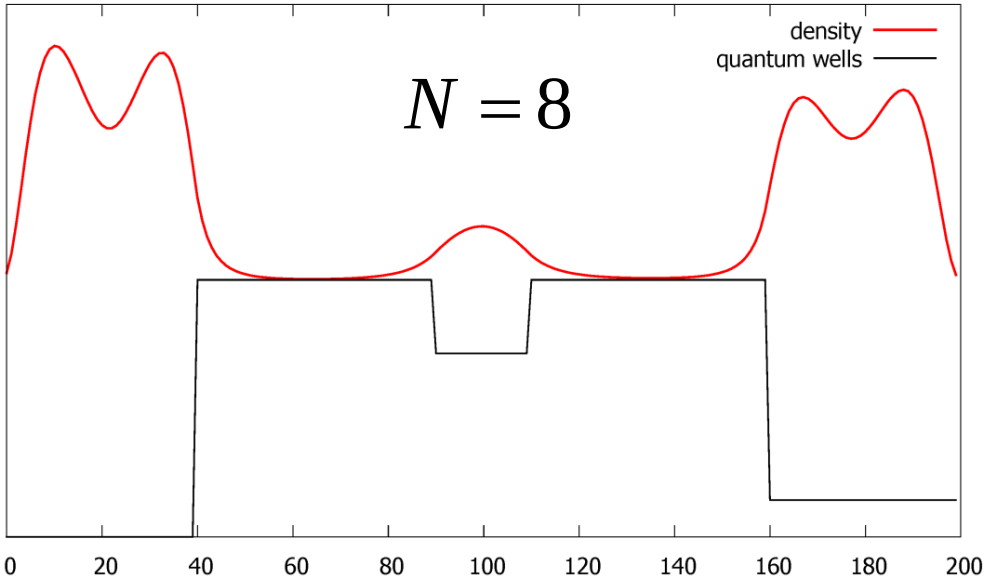

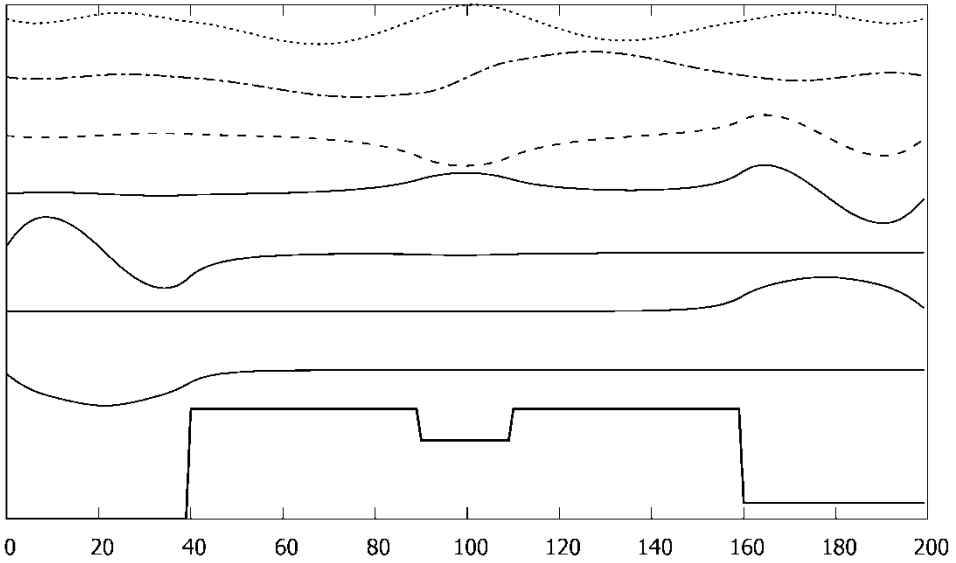

PHM: 1D examples

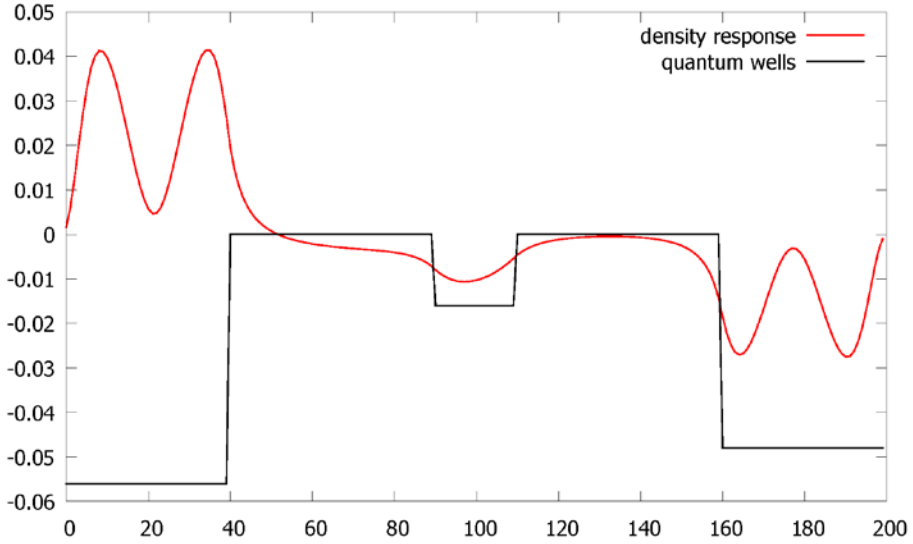

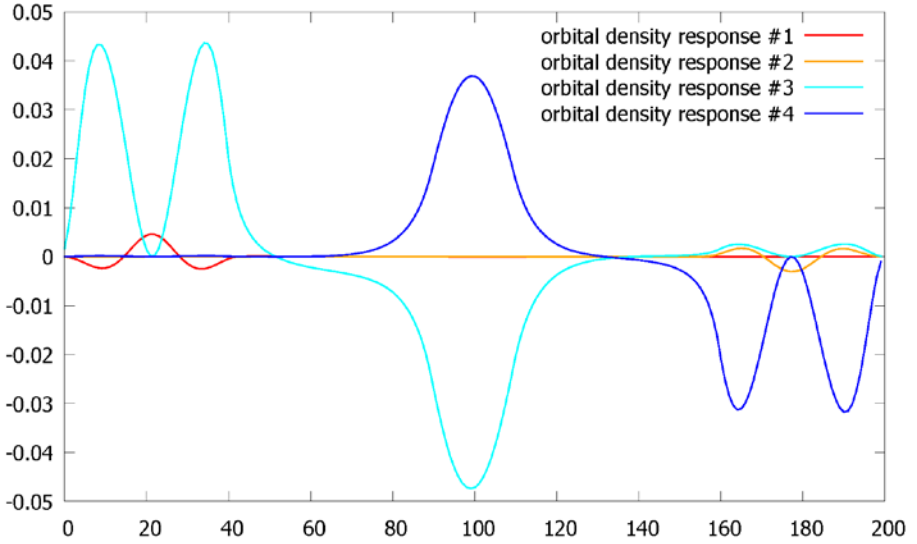

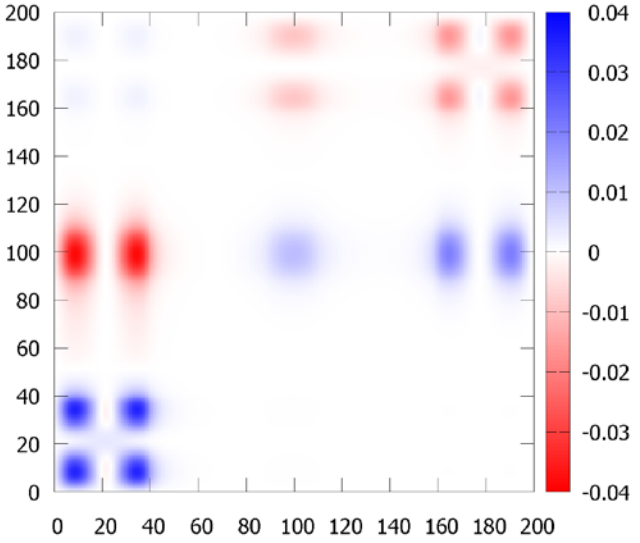

PHM

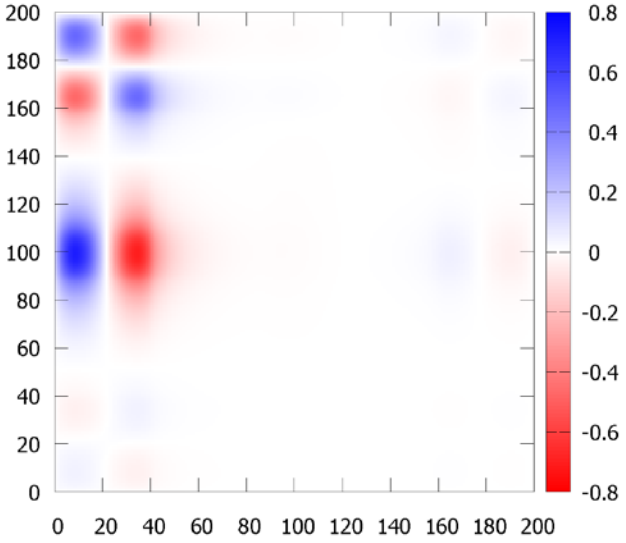

TDM

PHM: how to read it

integrates to δn in this direction

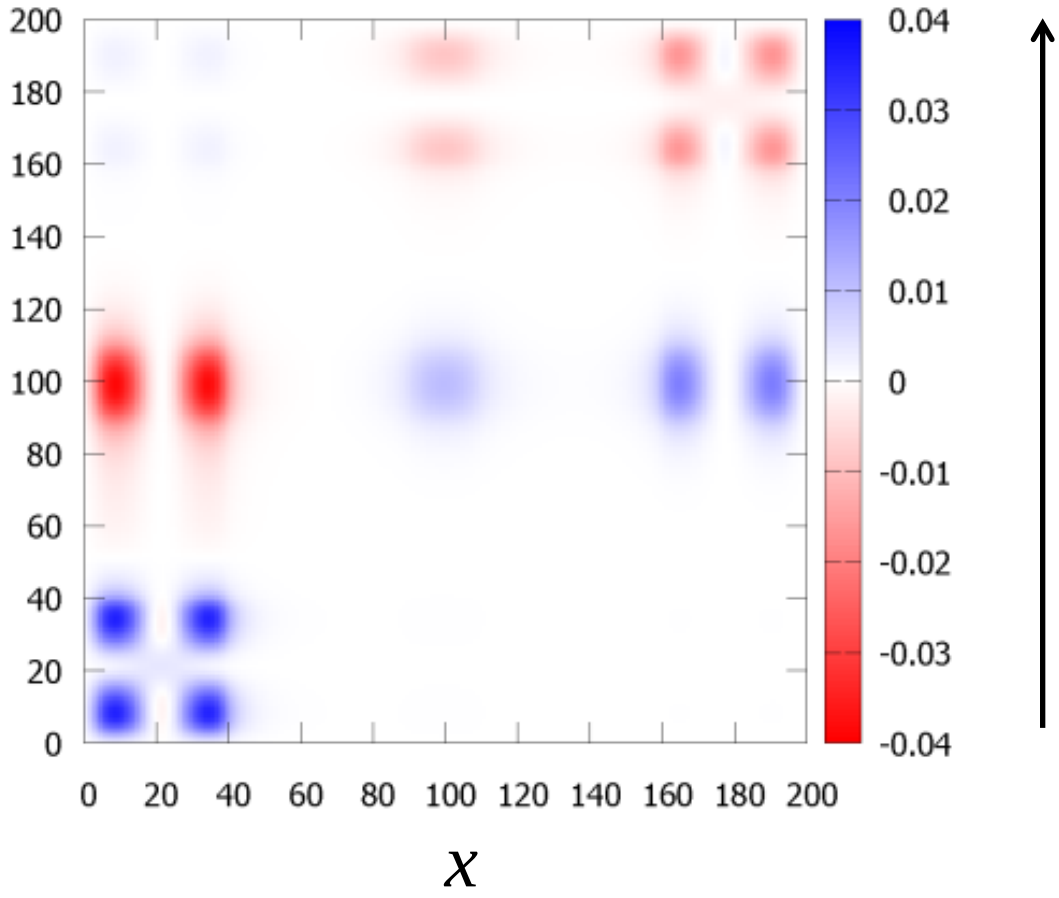

(where e/h is going to) x'

integrates to zero in this direction

x

(where e/h is coming from)

blue: electrons
red: holes

PHM: 1D examples

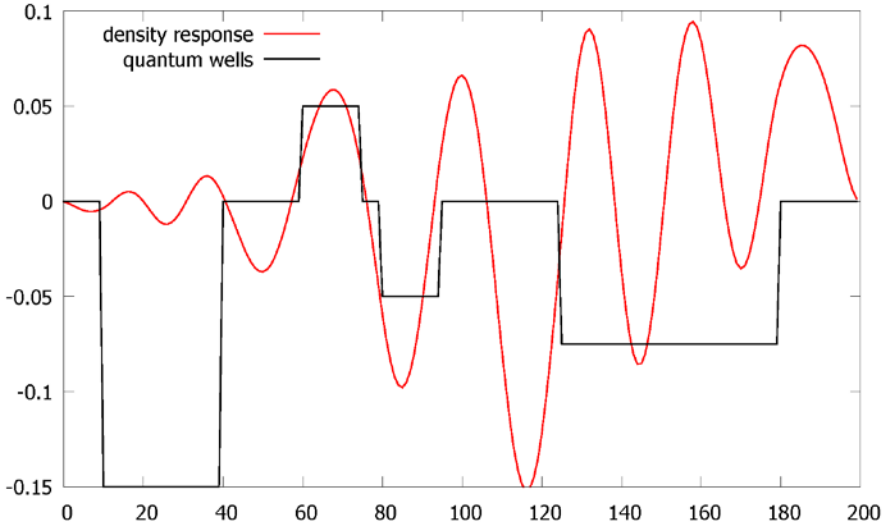

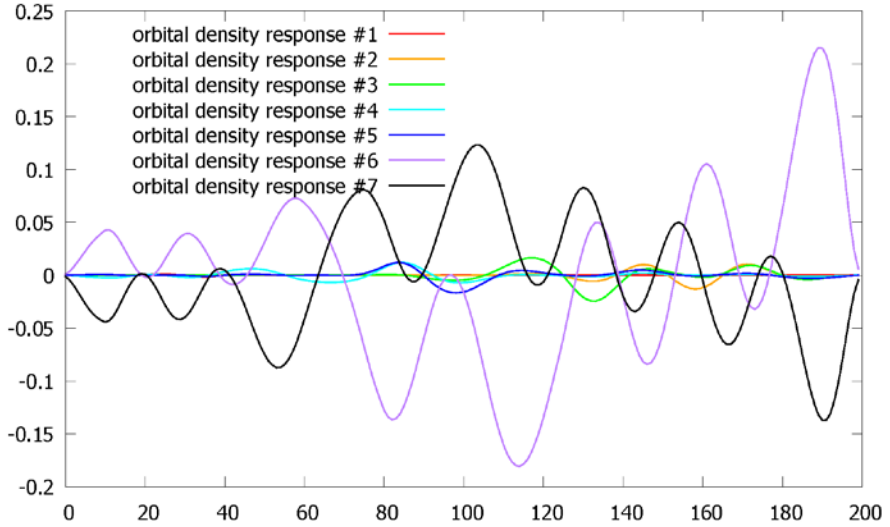

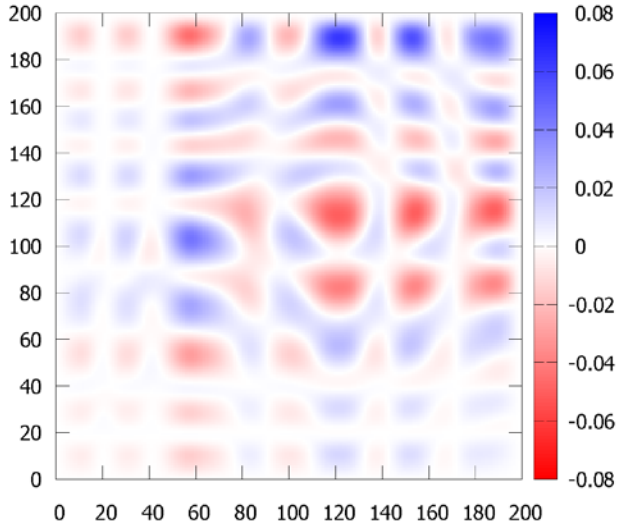

PHM

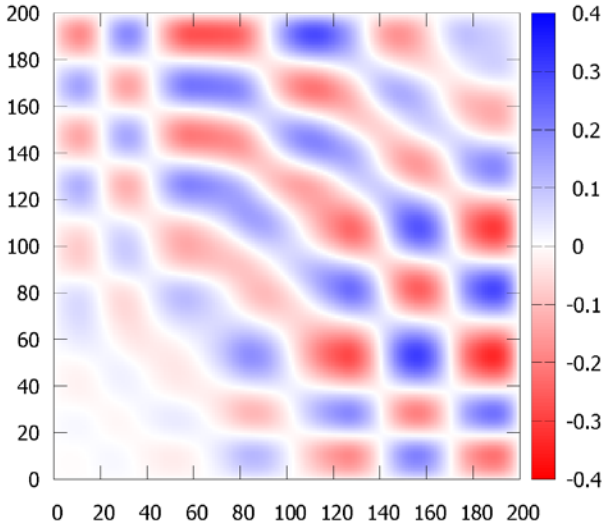

TDM

1D example: time-dependent PHM

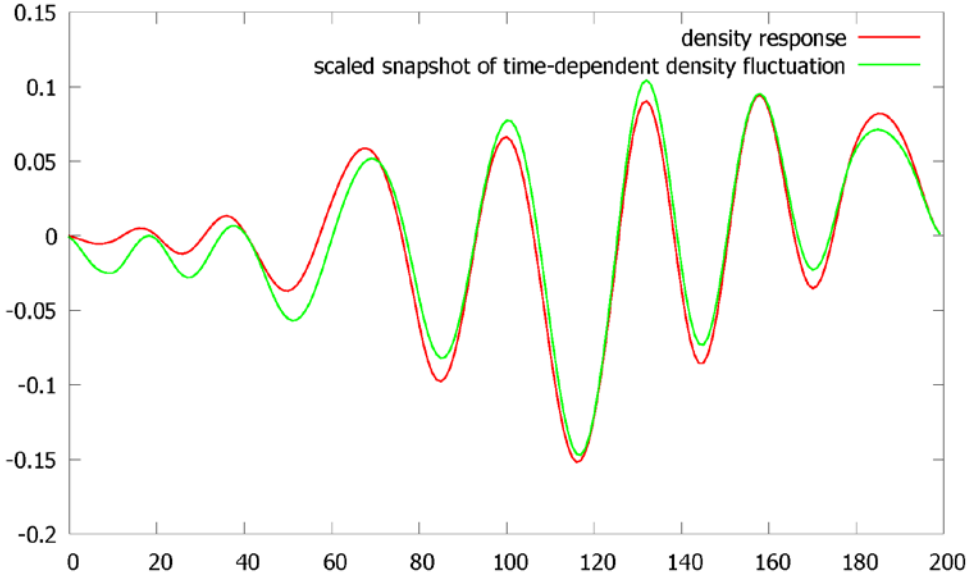

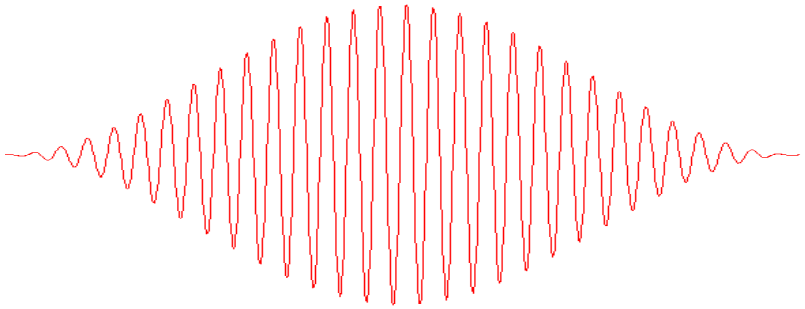

TDKS propagation, starting from ground state, with laser pulse at resonance

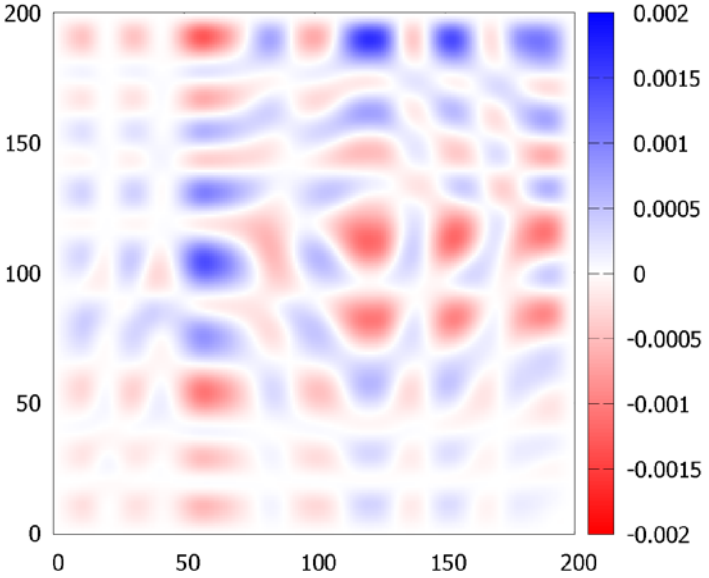

1DMol-dn.mp4

1DMol-outplane.mp4

The PHM in 3D: how to plot it

- Plot PHM for a fixed reference point: $\Xi(\mathbf{r}_0, \mathbf{r}', \Omega_n)$

- Atom-centered basis for KS orbitals: $\varphi_j(\mathbf{r}) = \sum_{l=1}^{N_A} \sum_{k=1}^{M_l} \varsigma_{jk}^{l} \eta_k^l(\mathbf{r})$

Assume zero overlap of basis functions on different atomic sites, and plot PHM similar to TDM as an array.

- For real-space grid, define a spatial coarse graining.

Each bin is numbered and we plot the average of the PHM over the bin. Can use boxes, slices, or Wigner-Seitz cells.

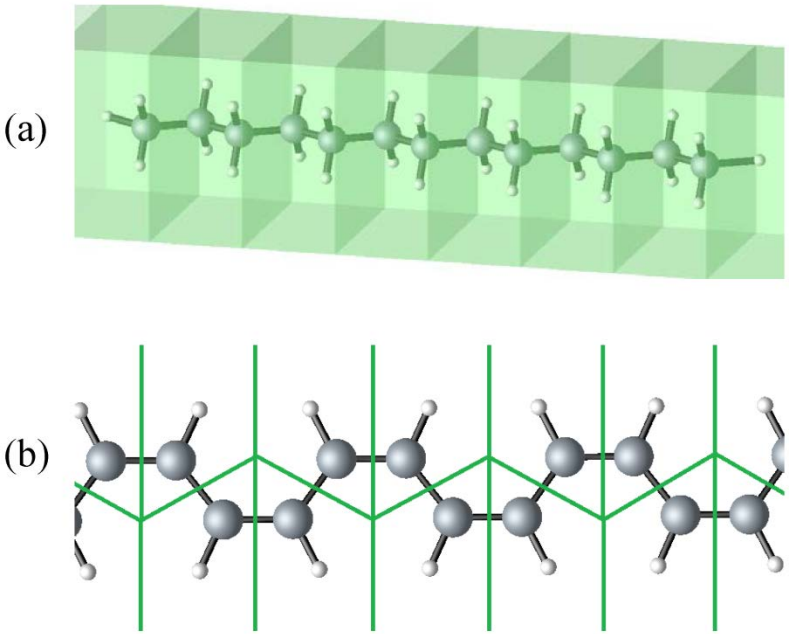

octopus

C_2H_4 – C_2F_4 charge transfer complex

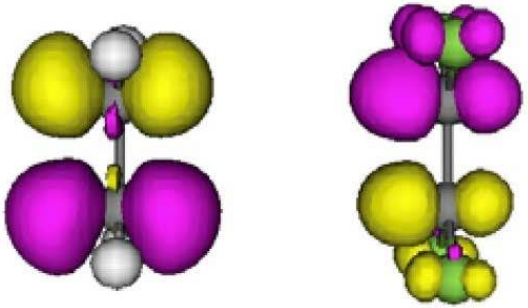

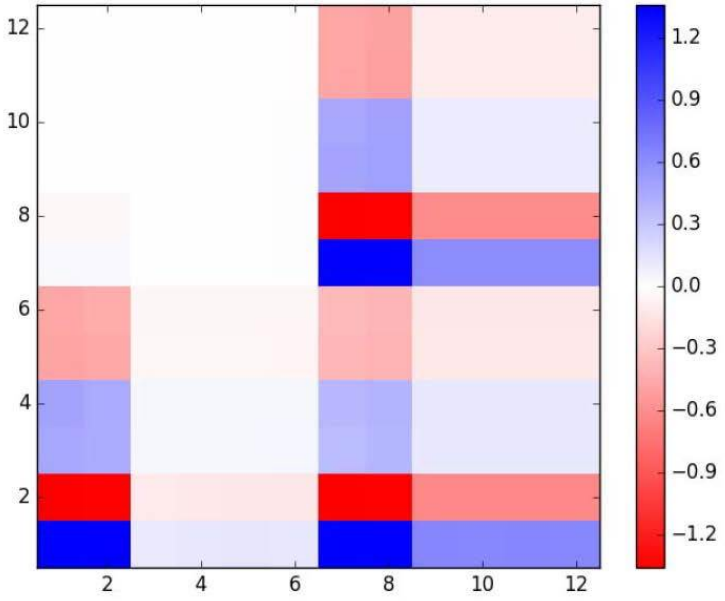

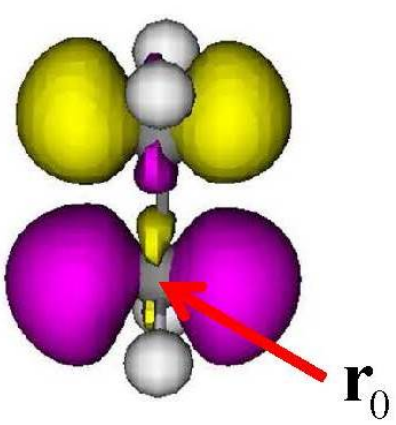

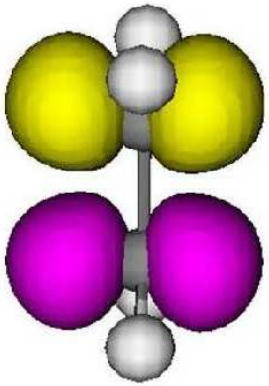

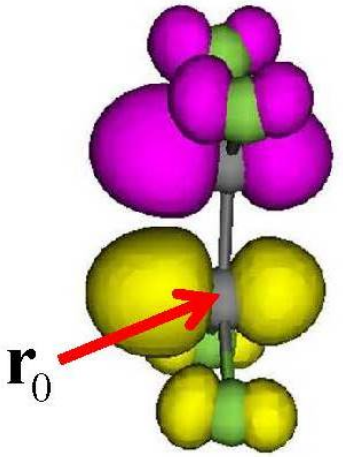

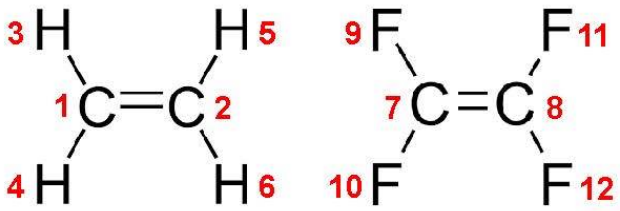

$$\Xi(\mathbf{r}_0, \mathbf{r}', \Omega_n)$$

PDPP-BBT versus TDPP-BBT

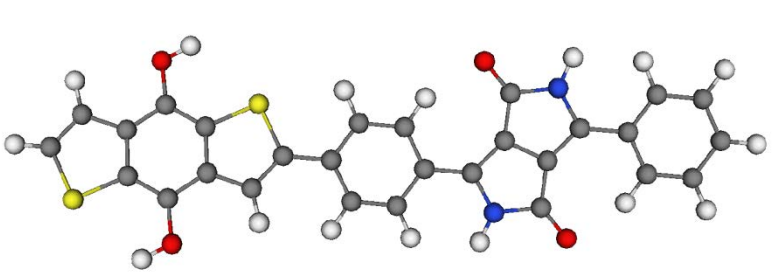

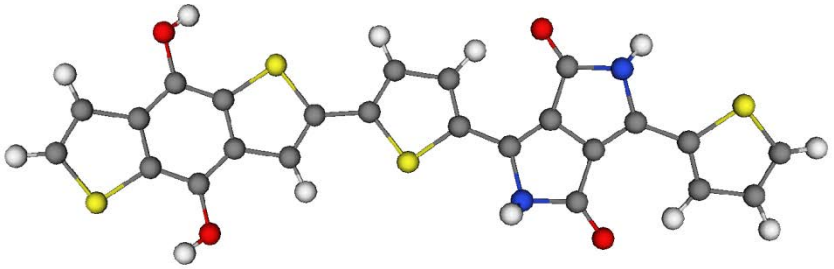

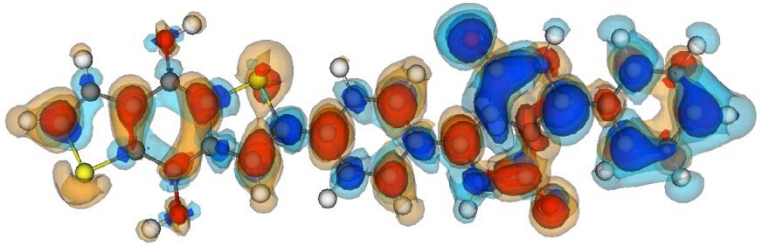

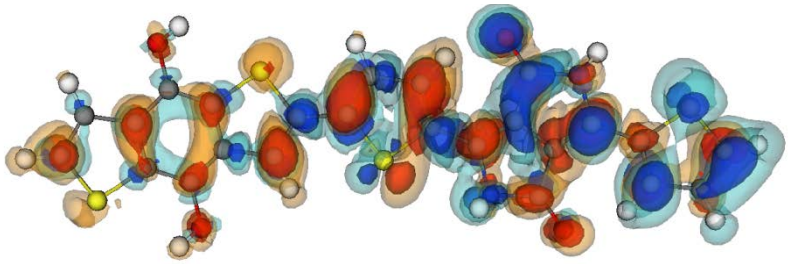

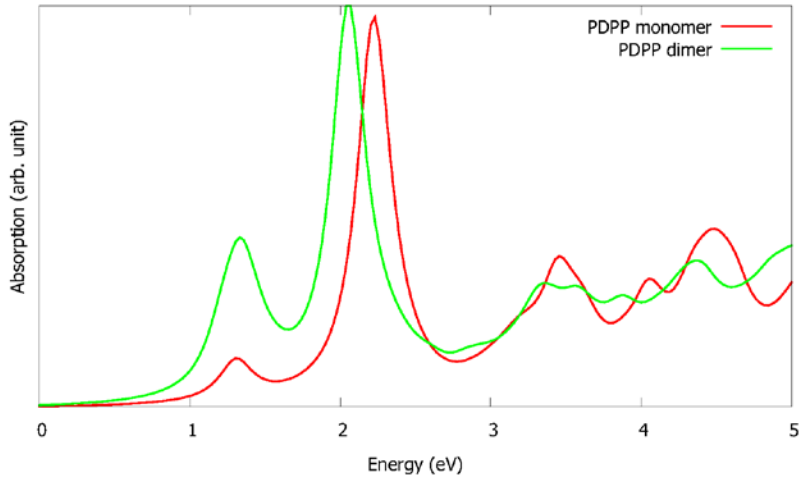

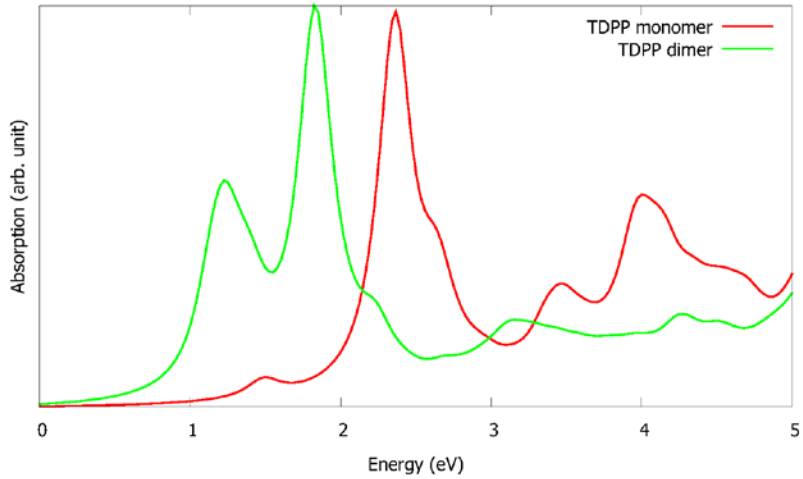

Both are donor-acceptor molecules, with very similar optical spectra. But TDPP has 20x bigger responsivity (photocurrent). Why?

PDPP-BBT versus TDPP-BBT: experiment

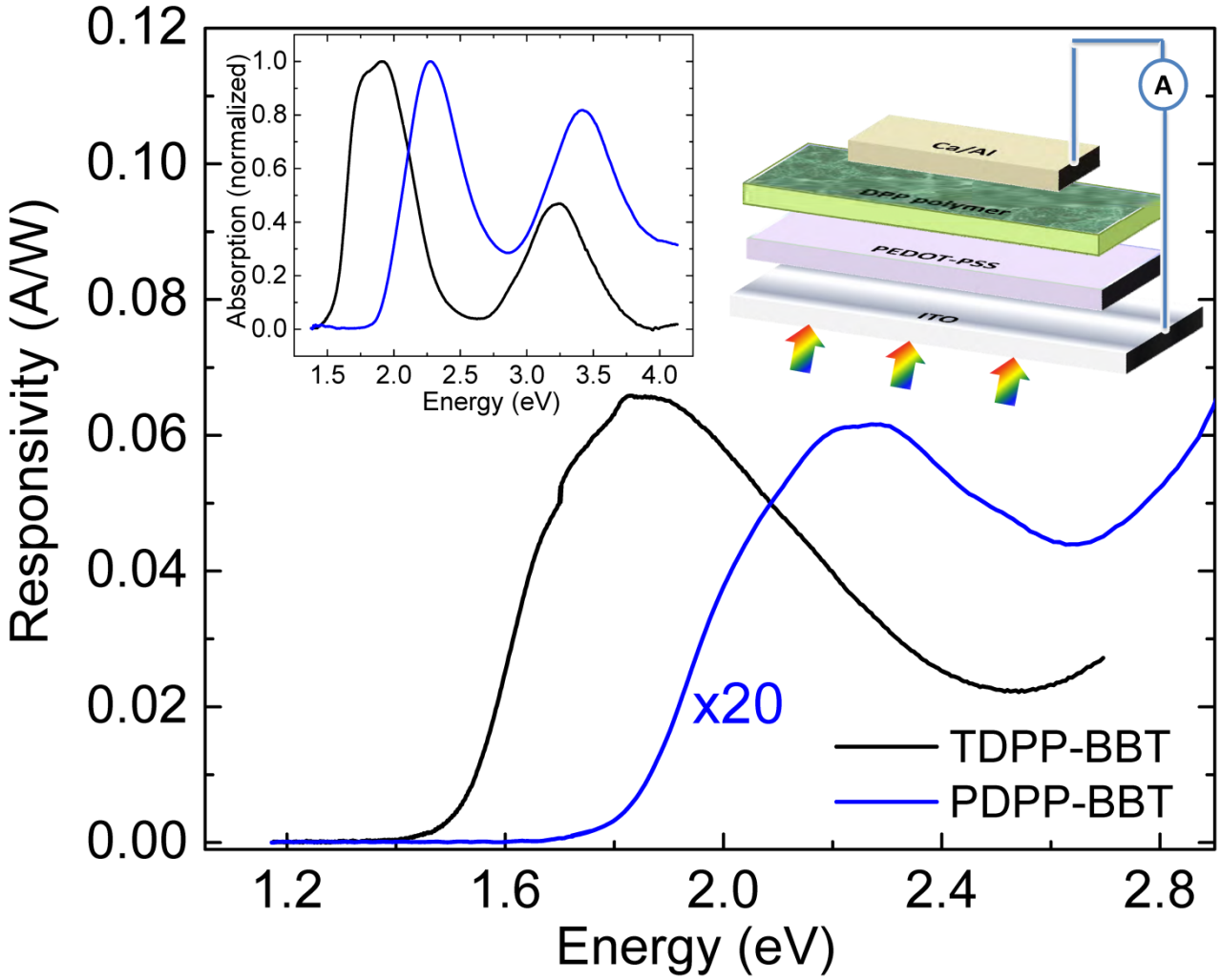

PDPP-BBT versus TDPP-BBT (monomers)

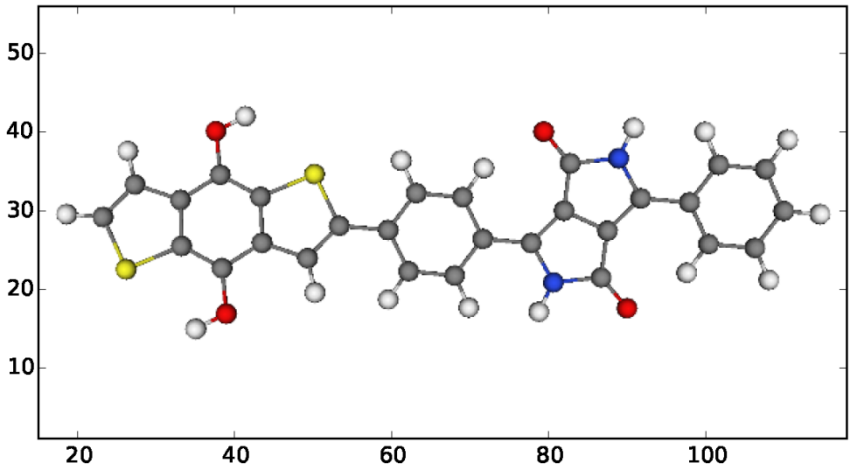

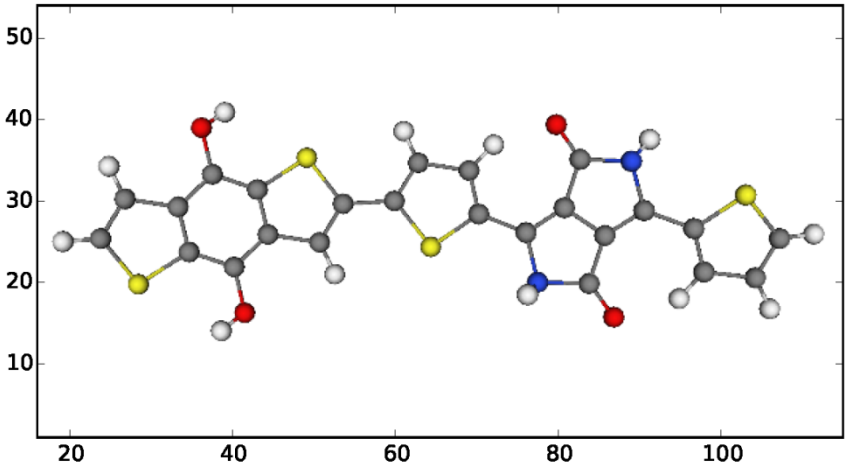

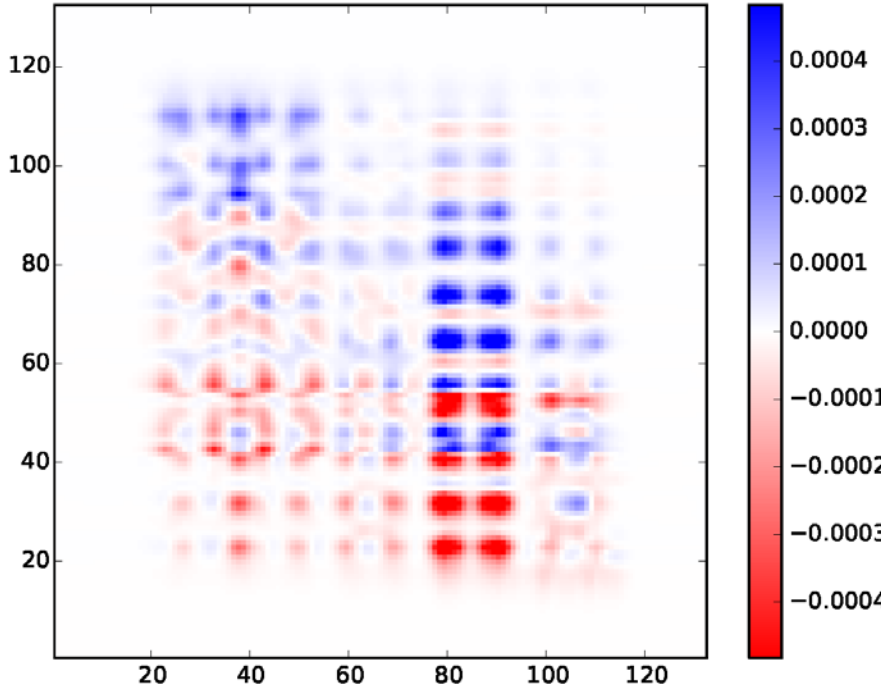

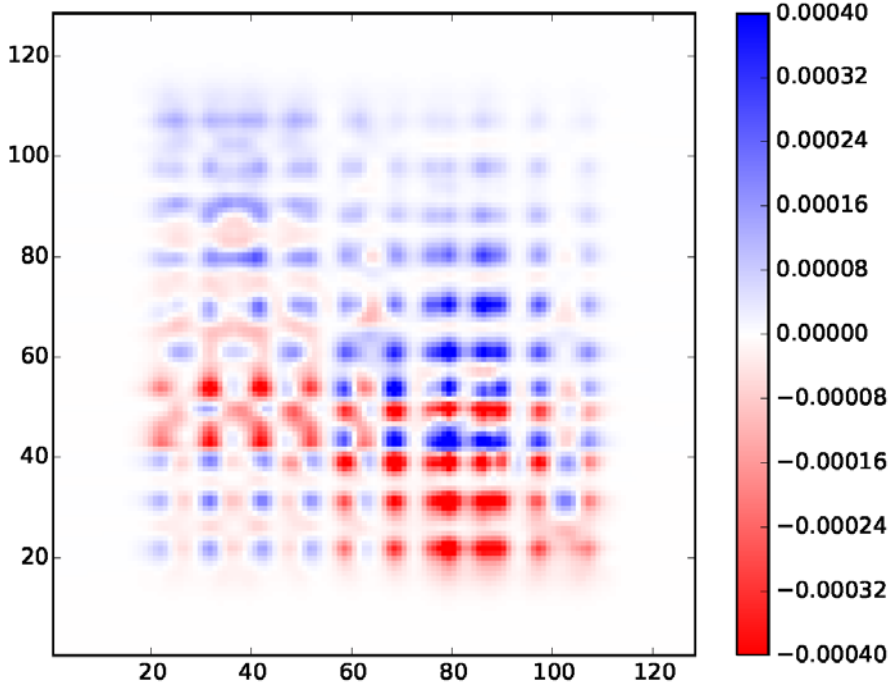

PDPP-BBT versus TDPP-BBT (dimers)

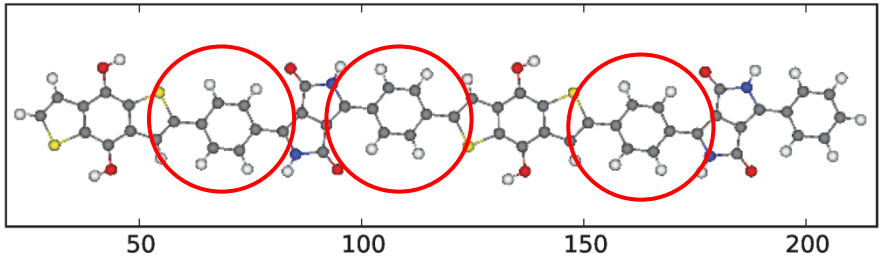

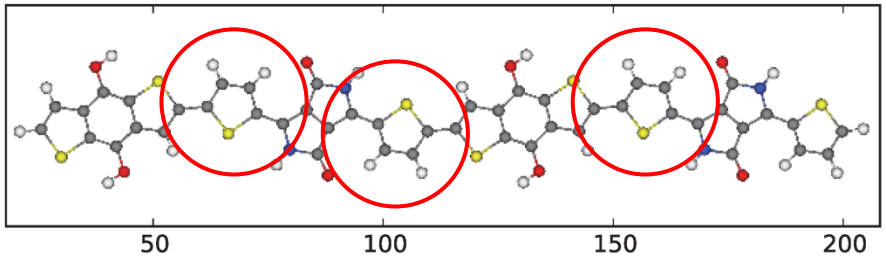

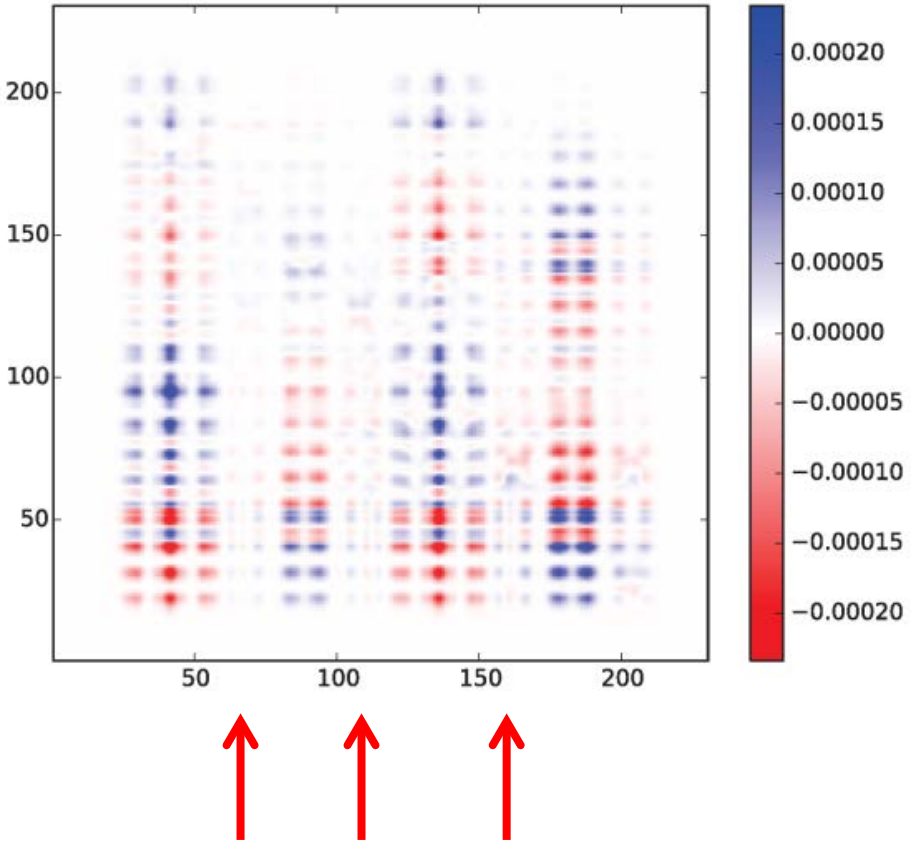

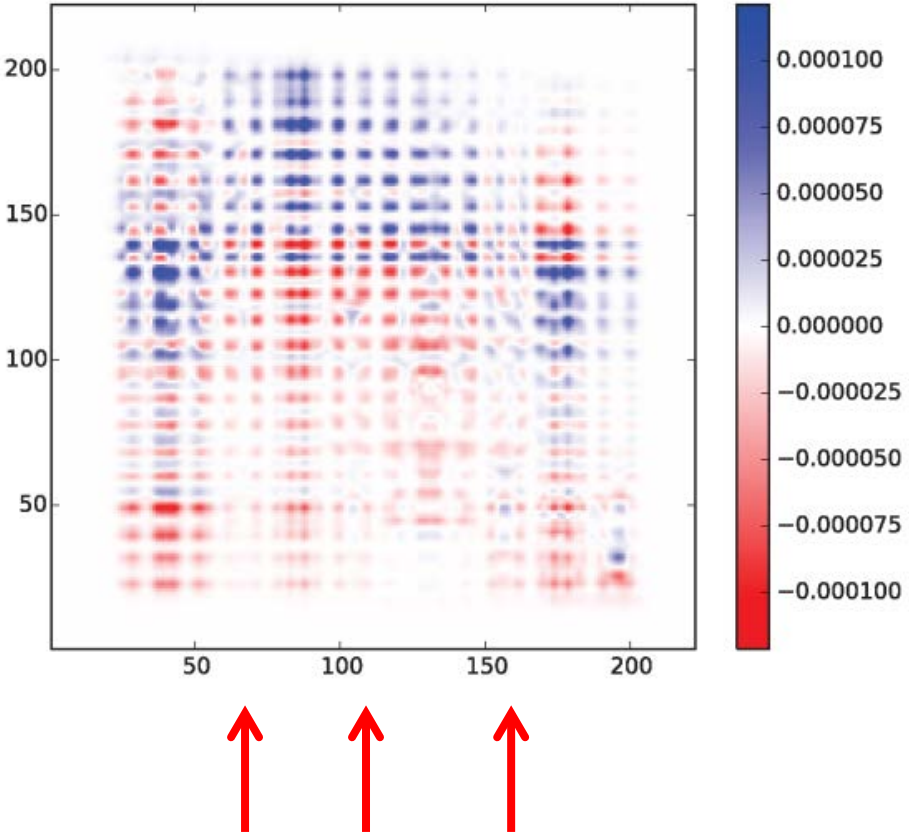

P3HT – C_{60} charge transfer complex

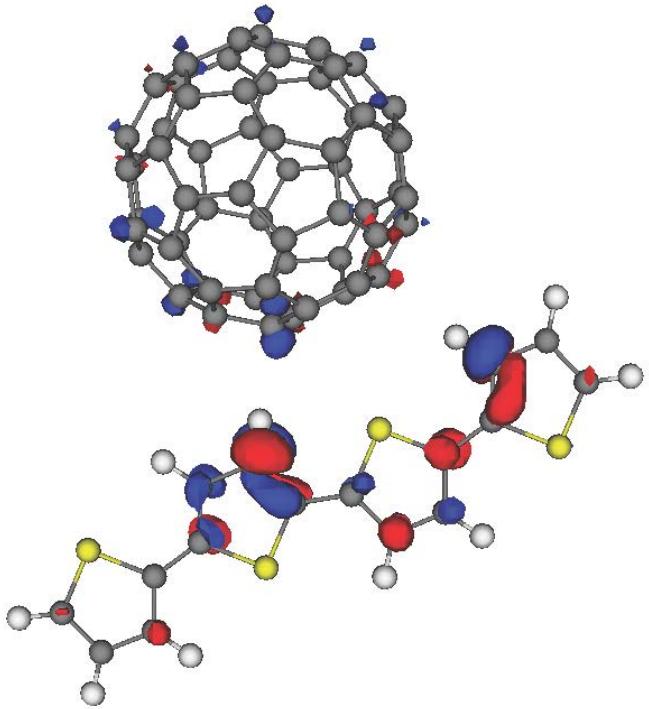

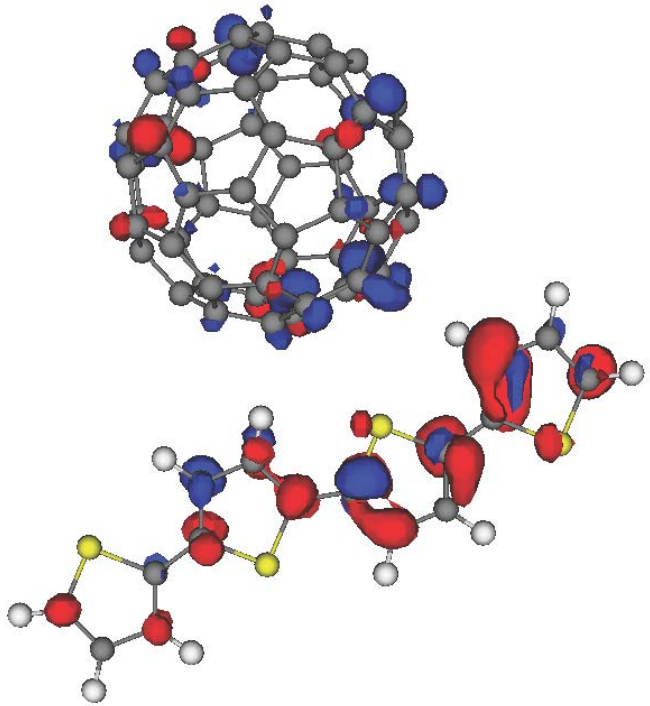

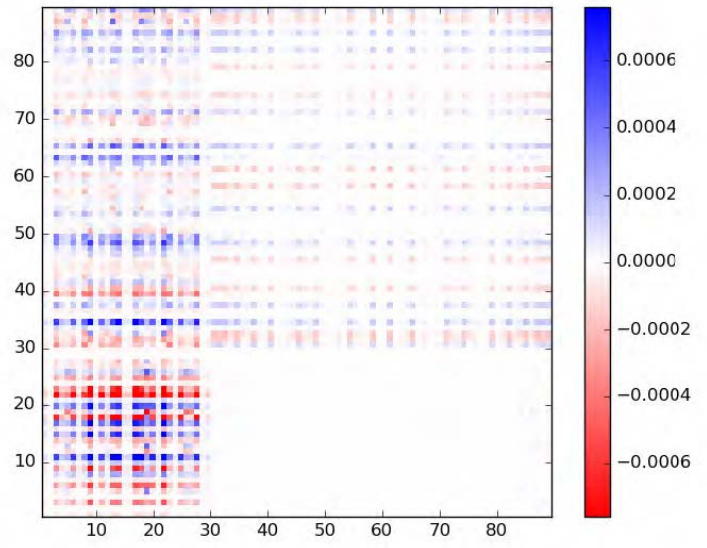

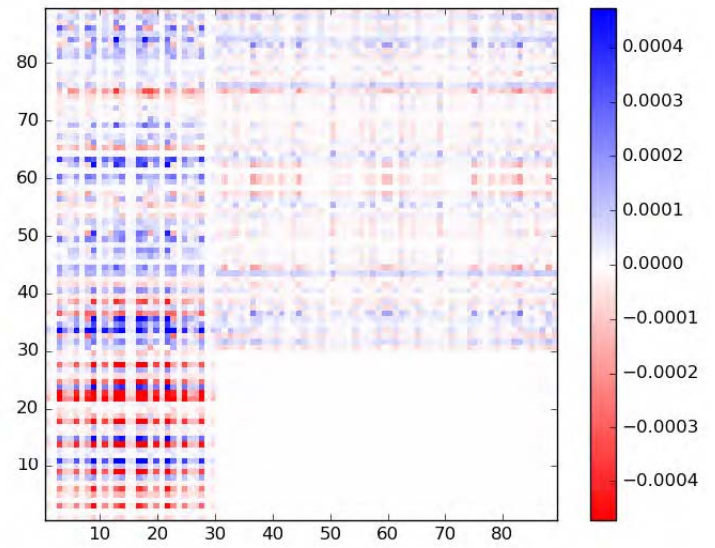

Extensions & Generalizations

Straightforward extensions:

- Moving nuclei
- Spin-dependent
- Ultrafast time-dependent (weak intensity)
- Strong excitations: can use $P(\mathbf{r},\mathbf{r}',t)$

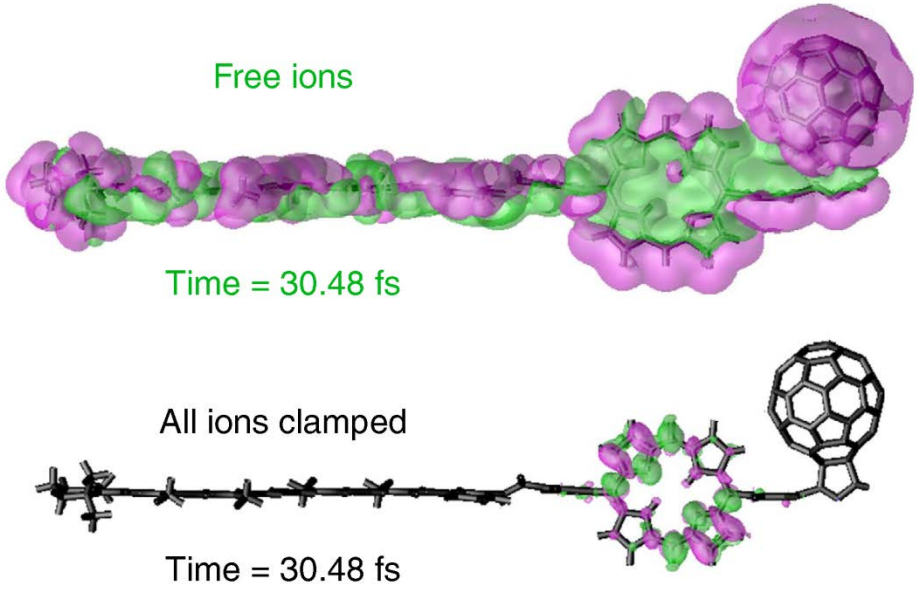

Rozzi et al., Nature Commun. (2015)

Bound excitons in periodic systems

2-band tight-binding model

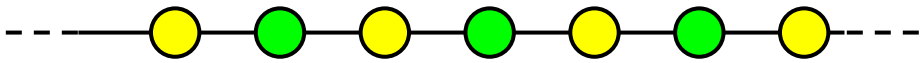

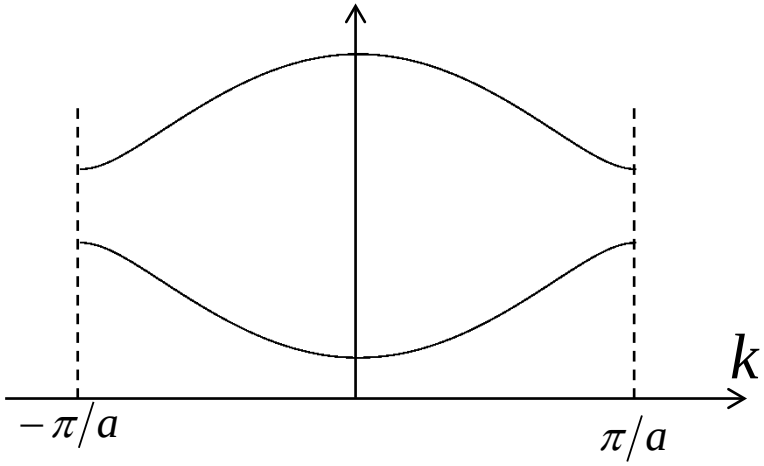

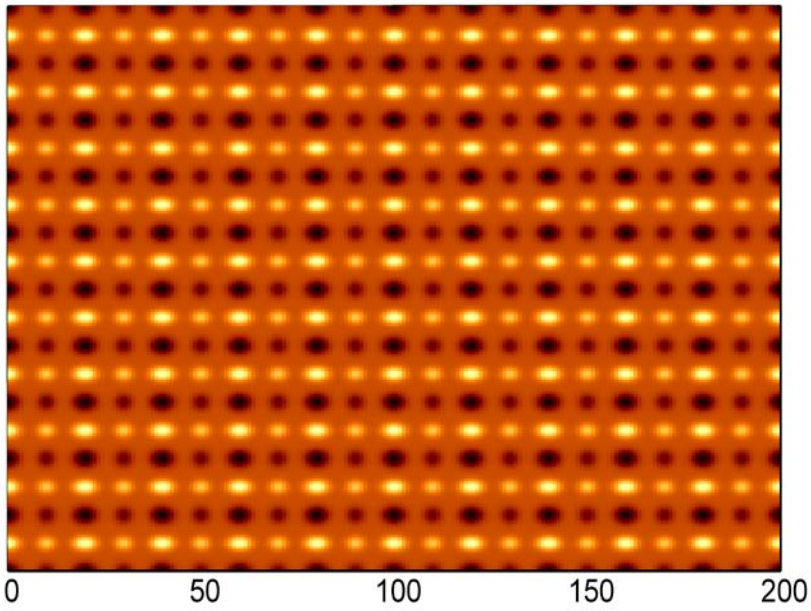

PHM

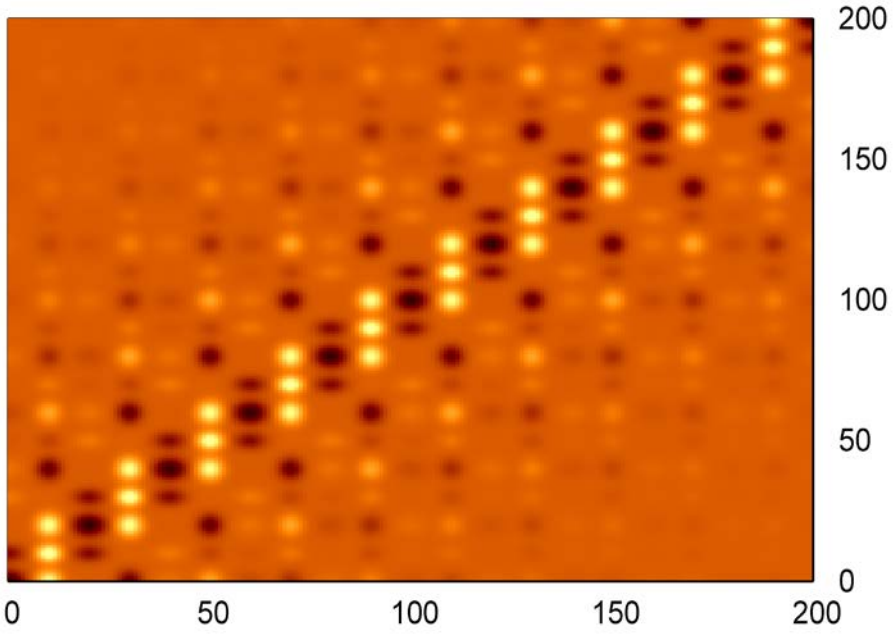

TDM

Z.H. Yang, Y. Li, and C.A. Ullrich, J. Chem. Phys. **137**, 014513 (2013)
Z.H. Yang, F. Sottile, and C.A. Ullrich, Phys. Rev. B **92**, 035202 (2015)

LiF

5x5 supercell

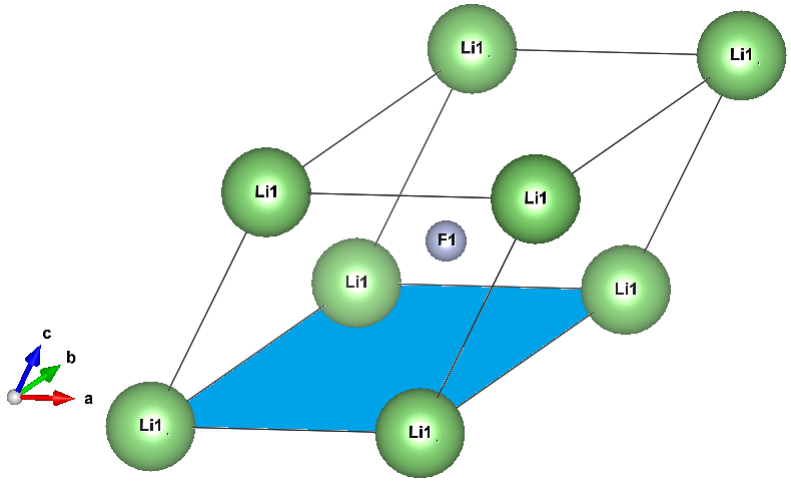

$|EWF|^2$

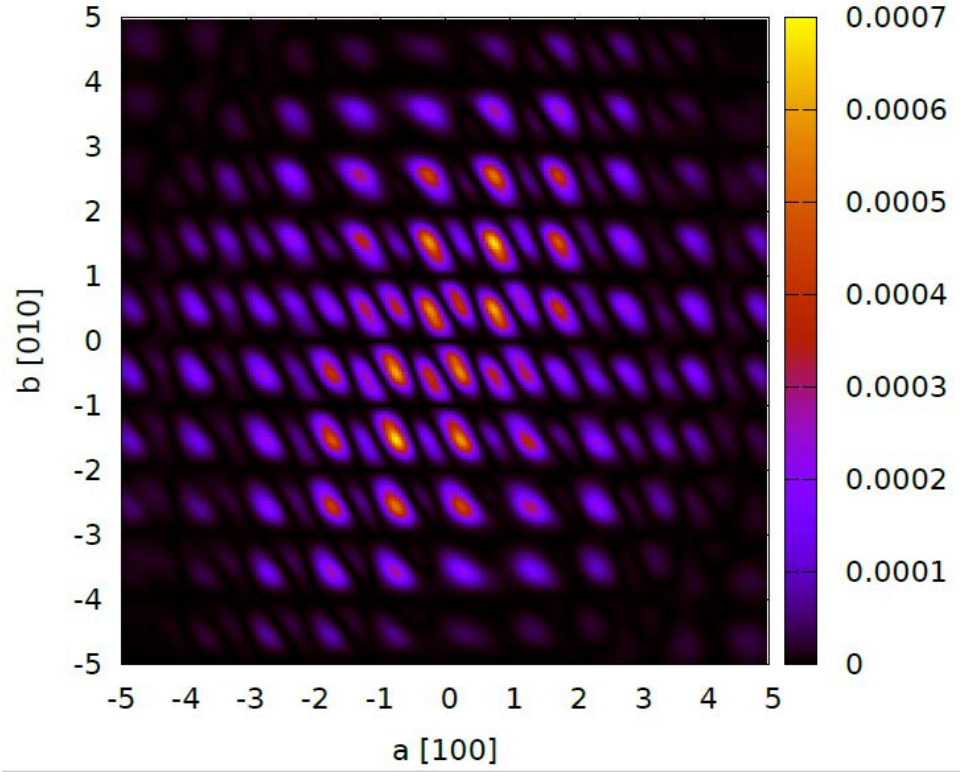

$|PHM|^2$

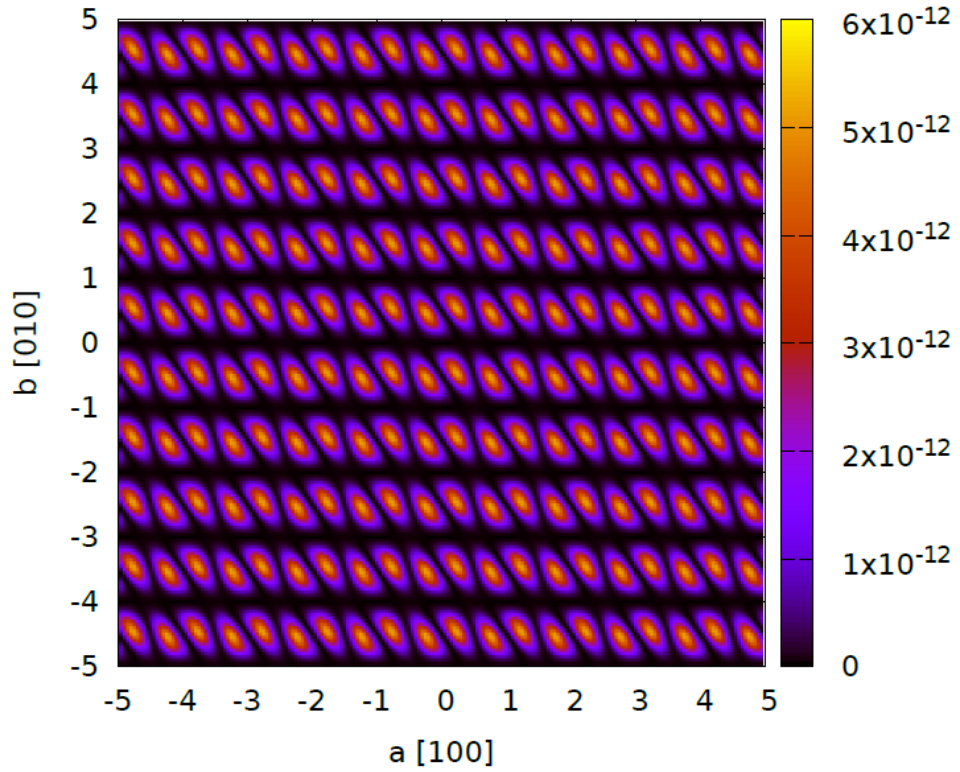

Summary

- TDM provides image of exciton wave function.
- PHM is ideal for charge-transfer processes. It can tell us
  - where electrons and holes are coming from and where they are going to
  - the role of individual chemical units in the excitation process
- Both are easy to apply as a post-TDDFT utilities, and provide complementary information
- Can be applied in real time to illustrate excitation dynamics.
- Applications in the ultrafast strong-field regime are possible

Y. Li and C.A. Ullrich, Chem. Phys. **391**, 157 (2011)
Y. Li and C.A. Ullrich, J. Chem. Theory Comput. **11**, 5838 (2016)
Y. Li, D. Moghe, S. Patil, S. Guha, and C.A. Ullrich, Mol. Phys. **114**, 1365 (2016)
Y. Li and C.A. Ullrich, submitted to JCP (2016)